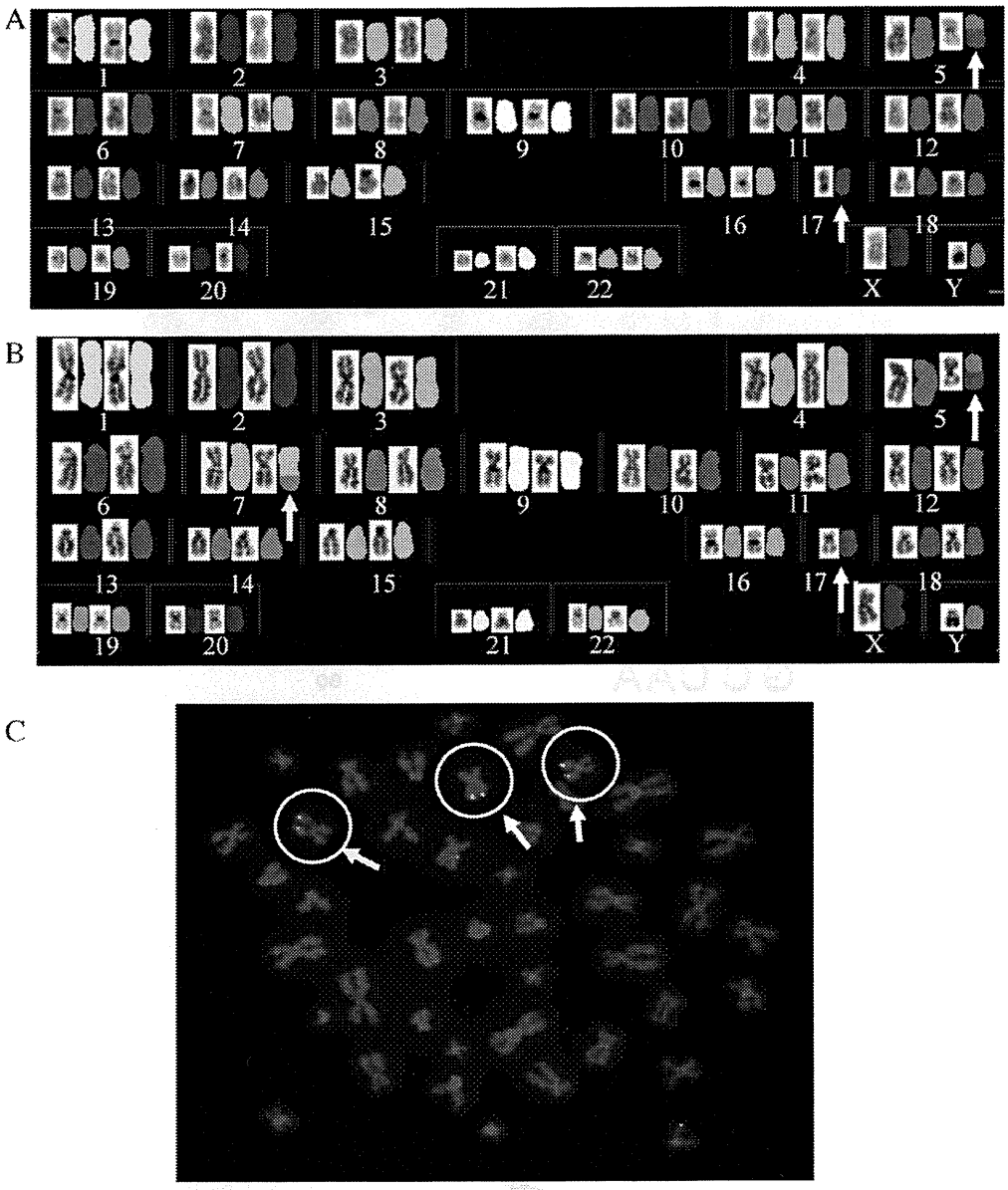

Fig. 2. der(7)t(7;11) and *MLL* gene duplication in GM colony-constituent cells grown from CD34+ BM cells at onset under stimulation with a combination of hematopoietic growth factors in patient no. 6. (A and B) Sky analysis revealed that one of three GM colony-constituent cells possessed der(5;17) and the remaining 2 cells had both der(5;17) and der(7)t(7;11). (C) FISH analysis revealed 3 signals for *MLL* in 4 of five GM colony-constituent cells.

cells. The cut-off value of 1 signal for the *TP53* gene was defined as the mean + 2 S.D. obtained from normal controls.

2.5. Spectral kayotyping

Spectral karyotyping (SKY) analysis was performed according to the instructions provided with the SKY probe kit (Applied Spectral Imaging, Carlsbad, CA), as reported previously [22]. An SD200 Spectracube (Applied Spectral Imaging) was used for image acquisition.

2.6. Clonal cell culture

Clonal cell cultures were carried out in a dish containing methylcellulose medium supplemented with granulocyte-macrophage (GM) colony-stimulating factor, stem cell factor, interleukin-3, and erythropoietin (Methocult GF H4434, Stemcell Technologies Inc., Vancouver, Canada). Dishes were incubated at 37 °C in a humidified atmosphere with 5% CO_2. On day 14, GM colonies and erythroid colonies were individually lifted and prepared as single-cell suspensions, as described previously [12]. Then, sequence and FISH analyses were performed on GM or erythroid colony-constituent cells.

3. Results

3.1. TP53 gene analysis and immunohistochemical analysis of p53 in patients with MDS

We performed *TP53* gene analysis and immunohistochemical analysis of p53 in 6 patients with *de novo* MDS (cases no. 1, 2 and 4–7), one patient with therapy-related MDS (case no. 3), and 2 patients with AML with myelodysplasia-related changes (cases no. 8 and 9). As presented in Table 1, all of them had chromosomal abnormalities such as monosomy 7 and trisomy 8. Among 9 patients, one patient (case no. 6) exhibited deletion and mutation of the *TP53* gene. According to immunostaining, approximately 20% of his BM cells on paraffin-embedded sections (Fig. 1A) or half of his BM mononuclear cells spread on glass slides showed profound overexpression of p53.

Please cite this article in press as: Saito S, et al. Genetic analysis of *TP53* in childhood myelodysplastic syndrome and juvenile myelomonocytic leukemia. Leuk Res (2011), doi:10.1016/j.leukres.2011.06.027

Table 1
Karyotypic and genetic abnormalities in bone marrow or peripheral blood mononuclear cells of 27 patients with MDS or JMML.

Case (no.)	Age (y)/Sex	WHO type	Karyotype (G-banding)	TP53 gene		p53 overexpression (cy to spin)	Mutations			
				Deletion	Mutation		PTPN11	KRAS	NRAS	Others
1	10/M	RCC	47,XY,+8[6], 46,XY[13]	–	–	1.0%	wt	wt	wt	–
2	1/F	RCC	47,XX,+6,add(11)(q13)[4],46,XX[17]	–	–	ND	wt	wt	wt	–
3	14/M	t-MDS	46,XY,der(7)t(1;7)(q12;q11)[6] 46,X,del(Y)(q11.2), der(21)t (1;21)(q25;q22) [5], 46,XY[8]	–	–	1.0%	wt	wt	wt	–
4	17/M	RCC→RAEB-2	45,XY,-7[19]	–	–	3.0%	wt	wt	wt	–
5	13/M	RAEB-2	47,XY,+X[18]	–	–	0.5%	1508G>T	wt	wt	–
6	1/M	RAEB-1→AML-MRC	45,XY,der(5;17)(p10;q10)[17], 46,XY[3]	51.6%	410T>A	51.5%	wt	wt	wt	–
7	3/F	RAEB-2	46~48,XX,-7,+8,add(9)(p24), add(18)(q21),+19,+r[cp21]	–	–	ND	wt	wt	wt	–
8	4/F	AML-MRC	47,XX,+8[19]	–	–	0.5%	227A>C	wt	wt	–
9	5/M	AML-MRC	45,XY,-7[18]	–	–	0.5%	1508G>A	wt	wt	FLT3-ITD
10	2/F	JMML	46, XX	–	–	0.5%	182A>T	wt	wt	–
11	0/M	JMML	ND	–	–	0.0%	214G>A	wt	wt	–
12	4/M	JMML	46,XY	–	–	2.5%	226G>A	wt	wt	–
13	0/M	JMML	46,XY	–	–	1.5%	226G>A	wt	wt	–
14	2/F	JMML	46,XX	–	–	3.5%	226G>A	wt	wt	–
15	1/M	JMML	46,XY	–	–	1.5%	227A>G	wt	wt	–
16	5/M	JMML	46,XY	–	–	3.5%	227A>G	wt	wt	–
17	1/F	JMML	46,XX	ND	–	1.0%	wt	35G>A	wt	–
18	0/F	JMML	46,XX	–	–	0.0%	wt	35G>A	wt	–
19	0/F	JMML	46,XX	–	–	2.0%	wt	34G>A	wt	–
20	1/F	JMML	46,XX	ND	–	1.5%	wt	38G>A	wt	–
21	0/M	JMML	46,XY	–	–	1.0%	wt	wt	34G>A	–
22	0/M	JMML	46,XY	–	–	1.5%	wt	wt	34G>A	–
23	1/F	JMML	46,XX	–	–	1.0%	wt	wt	35G>A	–
24	2/M	JMML	46,XY	–	–	1.0%	wt	wt	35G>A	–
25	0/F	JMML	46,XX	–	–	1.0%	wt	wt	38G>A	–
26	0/M	JMML(NF1)	47,XY,+8[2], 46,XY[18]	–	–	1.5%	wt	wt	wt	–
27	3/M	JMML(NF1)	46,XY	–	–	1.0%	wt	wt	wt	–

Since 0.94 ± 0.43% (0–1.81%) of bone marrow or peripheral blood mononuclear cells had 1 signal for TP53 gene in 17 normal controls, the cut-off value of TP53 deletion was defined as 1.8%. Since 1.25 ± 1.18% (0–3.6%) of PB mononuclear cells spread on glass slides were stained with anti-p53 monoclonal antibody in 6 normal controls, the cut-off value of p53 overexpression was defined as 3.61%. AML-MRC, AML with myelodysplasia-related changes; F, female; FISH, fluorescence in situ hybridization; FLT3-ITD, FMS-like tyrosine kinase 3 internal tandem dupulication; JMML, juvenile myelomonocytic leukemia; M, male; ND, not detected; NF1, neurofibromatosis type 1; RAEB, refractory anemia with excess blasts; RCC, refractory cytopenia of childhood; t-MDS, therapy-related myelodysplastic syndrome; wt, wild type.

Please cite this article in press as: Saito S, et al. Genetic analysis of *TP53* in childhood myelodysplastic syndrome and juvenile myelomonocytic leukemia. Leuk Res (2011), doi:10.1016/j.leukres.2011.06.027

3.2. Clinical and genetic characteristics of case no. 6 with deletion and mutation of *TP53* gene

Case no. 6 was an 18-month-old boy who was admitted to our hospital in June 2007 because of a leukocyte count of 5.87×10^9/l with 1% blasts, a hemoglobin level of 10.1 g/dl, and a platelet count of 33×10^9/l. Coupled with the findings that 5.2% of BM nucleated cells were blasts, he was diagnosed with MDS (refractory anemia with excess of blasts-1). He had a markedly short stature and mental retardation, but no first-degree relatives with malignancies (including breast carcinoma and leukemia) at an early age. According to G-banding analysis, 17 of 20 metaphase marrow cells revealed der(5;17)(p10;q10), and the remaining cells did normal karyotype. Spectral karyotyping (SKY) analysis on GM colony- and erythroid colony-constituent cells grown with hematopoietic growth factors confirmed the same chromosomal abnormality (Fig. 2A). On the other hand, PB mononuclear cells stimulated with phytohemagglutinin were of normal karyotype. Deletion of the *TP53* gene was found in half of BM cells by means of FISH analysis with a probe for the *TP53* locus (Fig. 3). As presented in Fig. 1B, direct sequencing revealed the presence of heterozygous *TP53* mutation (410 T>A) in BM and PB cells, but not in nail. The *TP53* mutation was not detected in PB leukocytes 9 and 13 months before the diagnosis of MDS. PB cells of his father and mother showed wild-type *TP53* gene. The patient possessed the wild-type *NRAS*, *KRAS*, *PTPN11*, *CBL*, *FMS-like tyrosine kinase-3 receptor*, *c-kit*, *CSF1R*, *BRAF*, *IDH1*, and *IDH2* genes. He did not have the clinical features of neurofibromatosis type I. Additionally, the chromosomal breakage test using diepoxybutane and mitomycin C on PB lymphocytes was negative. Serum trypsinogen and lipase levels were normal, and computed tomography scan showed no pancreatic lipomatosis. After a preparative regimen of total body irradiation, fludarabine, and cyclophosphamide, BM transplantation (BMT) from HLA-matched unrelated donor was performed in December 2008. Since grade III acute GVHD occurred on day 67, he was treated with tacrolimus and methylprednisolone. Since short tandem repeat-PCR detected reappearance of a recipient-specific allelic signal on day 197, the first course of donor lymphocyte infusion was administered. However, on day 252, his BM cells were found to contain 24% blasts positive for CD13, CD33, CD34, CD41, and CD71. Three more courses of donor lymphocyte infusion combined with chemotherapy resulted in only temporary stabilization of the disease. A second BMT from his HLA-haploidentical mother was performed 441 days after 1st BMT, but he died on 134 days after 2nd BMT because of disease progression.

To elucidate whether or not the *TP53* gene abnormalities were restricted to the myeloid lineage, we performed cytogenetic analysis of circulating myeloid, B, and T cells obtained at diagnosis. $CD14^+/CD15^+$ PB cells possessed homozygous *TP53* mutation according to direct sequencing (Fig. 1C). FISH analysis revealed loss of one *TP53* allele in 90% of the $CD14^+/CD15^+$ cells. On the other hand, $CD19^+$ and $CD3^+$ PB cells possessed the wild-type of *TP53* gene. In addition, a large proportion of both lymphocytes had 2 signals for the gene. To examine whether the *TP53* abnormalities occurred at the progenitor level, we picked up GM colonies and erythroid colonies grown from $CD34^+$ BM cells at onset under stimulation with a combination of hematopoietic growth factors. The *TP53* homozygous mutation was detected in all of 9 GM colonies and in all of 8 erythroid colonies. Moreover, 99 of 100 pooled GM colony-constituent cells and 98 of 100 pooled erythroid colony-constituent cells had 1 signal for *TP53*. Mutated *TP53* gene and a loss of *TP53* gene remained stable in BM cells after the first and second transplantations.

Since Anderson et al. [23] reported that 7 of 8 therapy-related MDS or AML patients with mutations of *TP53* had duplication or

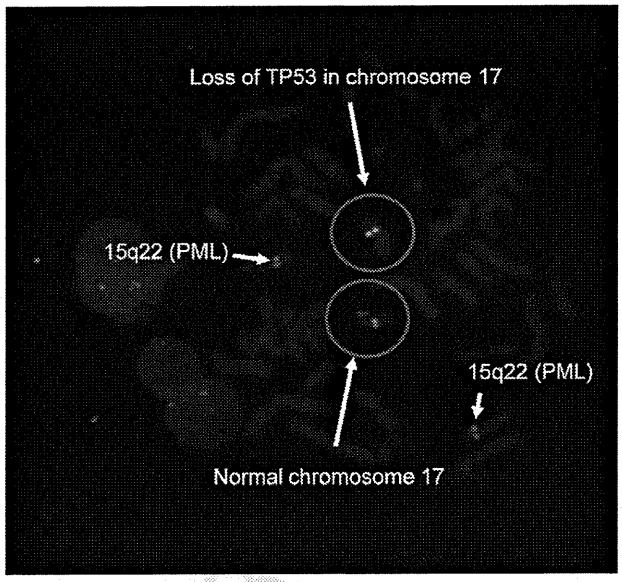

Fig. 3. FISH analysis of BM cells using *TP53*, *RARα*, and *PML* probes in patient no. 6. Half of BM cells had 1 signal for *TP53*. *TP53* on 17p13.1, red; *RARα* on 17q21, green; *PML* on 15q22, red. (For interpretation of the references to color in this figure legend, the reader is referred to the web version of the article.) Q1

amplification of the *MLL* gene, we examined the *MLL* gene copy number before and after BMT. FISH analysis revealed that only 1% of pre-transplant PB cells had 3 signals of the *MLL* gene in patient no. 6. The frequency of cells with extra copies of the *MLL* gene was 0.8%, and that of cells with 2 copies was 98% in 5 normal control PB cells. Interestingly, the der(7)t(7;11) as well as der(5;17) was found in 2 of three GM colony-constituent cells and in 4 of five erythroid colony-constituent cells grown from $CD34^+$ BM cells at onset under stimulation with hematopoietic growth factors according to SKY analysis (Fig. 2B). FISH analysis revealed 3 signals for *MLL* in 4 of five GM colony-constituent cells and in 65 of 100 erythroid colony-constituent cells (Fig. 2C). These results suggested the existence of the extra *MLL* gene on der(7)t(7;11). Eight months after the 1st BMT, FISH analysis revealed that 8% of BM cells had 3 signals for *MLL*. The frequency of PB cells with 3 *MLL* signals increased to 88% three months after the 2nd BMT.

3.3. *TP53* gene analysis and immunohistochemical analysis of p53 in patients with JMML

We then performed *TP53* gene analysis and immunohistochemical analysis of p53 in a total of 18 children with JMML (7 *PTPN11* mutations; 4, *KRAS* mutations; 5, *NRAS* mutations; 2, NF1 individuals). All JMML patients examined had neither *TP53* gene aberration nor p53 overexpression (Table 1).

4. Discussion

There have been a few reports regarding pediatric patients with hematologic malignancies who possessed *TP53* abnormalities. Felix et al. [6] demonstrated that only one patient showed a 2-base-pair deletion in the *TP53* gene among 19 children with therapy-related leukemia or MDS. The other investigators also described a lack or very small numbers of *TP53* aberrations in more than 30 pediatric MDS patients [18,24]. On the other hand, in a recent study of 19 pediatric MDS patients, 18 children (94.7%) had deletion of the *TP53* gene according to FISH analysis [7]. Our results supported the low frequency of the *TP53* abnormalities in childhood MDS. One

Please cite this article in press as: Saito S, et al. Genetic analysis of *TP53* in childhood myelodysplastic syndrome and juvenile myelomonocytic leukemia. Leuk Res (2011), doi:10.1016/j.leukres.2011.06.027

possible explanation for the major differences in the frequency of TP53 abnormalities among the reports is the different frequency of MDS patients with deletion involving 17p13.1. In JMML, the *TP53* aberrations do not appear to be related to leukemogenesis.

On the basis of markedly short stature and mental retardation in patient no. 6, we evaluated the possibility that hematological abnormalities are a manifestation of germline *TP53* mutation. DNA obtained from his nails and lymphocytes showed the wild type of the *TP53* gene, while DNA from myeloid cells revealed a point mutation. Thus, the patient appeared to have a somatic mutation, but not a germline mutation, in the *TP53* gene. Coupled with no history of malignancy in first-degree relatives, the patient did not fulfill the Chompret criteria for Li-Fraumeni syndrome. De Filippi et al. [25] reported a JMML patient with a constitutional mutation of *NRAS* gene who had short stature and some dysmorphic features. Niemeyer et al. [26] demonstrated a dominant developmental disorder resulting from germline missense *CBL* mutations, which is characterized by impaired growth, developmental delay, cryptorchidism and a predisposition to JMML. Nevertheless, these genes of patient no. 6 were of the wild-type. Additionally, he might not have had Schwachman-Diamond syndrome because of normal pancreatic function. However, we cannot exclude a possibility of germline mutation of genes other than those described above.

In patient no. 6, $CD14^+/CD15^+$ PB cells possessed homozygous *TP53* mutation, and 90% of them revealed loss of one *TP53* allele. All of 9 GM progenitors and all of 8 erythroid progenitors generated progenies with the *TP53* homozygous mutation. Additionally, a great majority of pooled GM or erythroid colony-constituent cells had 1 signal for p53. On the other hand, $CD19^+$ and $CD3^+$ PB cells had neither mutation nor deletion of the gene. These results imply that an abnormal clone with deletion of the *TP53* gene in one allele and mutation in the other allele originated from hematopoietic stem cells with the potential to differentiate into myeloid and erythroid lineages, but not the lymphoid lineage. The loss of 17p is often accompanied by a *TP53* mutation in AML and MDS [1,2]. It has been demonstrated that *TP53* mutations with or without a loss of one TP53 allele are strongly associated with a complex aberrant karyotype in AML and MDS, when compared with the values of the patients without a complex aberrant karyotype [3,27]. Since AML with markedly abnormal karyotypes may be genetically unstable, and contain a high frequency of point mutations in some genes, it is generally held that inactivation of *TP53* is mainly correlated with an advanced clinical stage [5]. In the contrast, in patient no. 6, der(5;17)(p10;q10) was recognized as the sole chromosomal abnormality at onset. Additionally, the *TP53* mutation was not detected in PB leukocytes at least 9 months before the diagnosis of MDS. Therefore, biallelic inactivation of the *TP53* gene might have played an important role in the occurrence of MDS in this case. Nevertheless, cooperation between loss of *p53* function and loss of a putative tumor suppressor gene at 5q cannot be excluded [28].

Serial FISH analyses showed that the abnormal clone with 3 copies of the *MLL* gene was at a negligible level before 1st BMT, but the clone became a major population of leukemic cells after the 2nd HSCT. Interestingly, according to the SKY and FISH analyses of cultured cells grown from $CD34^+$ BM cells under stimulation with hematopoietic growth factors, the patient had two clones at diagnosis: one clone with der(5;17), and the other clone with both der(5;17) and der(7)t(7;11), which appeared to contain the extra copy of the *MLL* gene. Taken together with our previous report on JMML patients who had 6-mercaptopurine-refractory clone [11], it is suggested that the minor clone with both *TP53* gene alteration and *MLL* duplication already existed at onset, and that poor outcome was associated with resistance of this clone to chemotherapy and radiation.

List of hospitals and people who cooperated in collecting clinical samples from the MDS and JMML patients

Hyogo Children's Hospital (K. Kawasaki, D. Hasegawa); Iwate Medical University (M. Endo); Kyoto University (S. Adachi); Kurashiki Central Hospital (M. Fujiwara); Gunma Children's Medical Center (M. Sotomatsu); University of Tsukuba (C. Kobayashi); Tenri Hospital (M. Okada); Toyama University (H. Kanegane); Dokkyo Medical University (K. Fukushima); Nagano Children's Hospital (H. Nagumo); Niigata Cancer Center (A. Ogawa, A. Watanabe); Hamamatsu Medical Center (Y. Mizuno, S. Yajima,); Hirosaki University (S. Sasaki).

Role of the funding source

This work was supported by Grants-in-Aid No. 2139008 from the Ministry of Education and by Grant-in-Aid for Cancer Research 16-3 from the Ministry of Health, Labour, and Welfare of Japan.

Conflict of interest

The authors disclose no actual or potential conflict of interest.

Acknowledgements

We thank Ms Yumiko Oguchi (Department of Pediatrics, Shinshu University School of Medicine) for the excellent technical assistance.

Contributions. K.K. and S.S. designed and performed research, analyzed data, and wrote the paper; K.M. designed and performed research, collected samples, analyzed data; C.T. and K.S. performed research and analyzed data; M.T-Y., R.Y., Y.N., K.S., and M.S. collected samples and analyzed data.

References

[1] Fenaux P, Jonveaux P, Quiquandon I, Laï JL, Pignon JM, Loucheux-Lefebvre MH, et al. P53 gene mutations in acute myeloid leukemia with 17p monosomy. Blood 1991;78:1652–7.
[2] Lai JL, Preudhomme C, Zandecki M, Flactif M, Vanrumbeke M, Lepelley P. Myelodysplastic syndromes and acute myeloid leukemia with 17p deletion. An entity characterized by specific dysgranulopoïesis and a high incidence of P53 mutations. Leukemia 1995;9:370–81.
[3] Haferlach C, Dicker F, Herholz H, Schnittger S, Kern W, Haferlach T. Mutations of the TP53 gene in acute myeloid leukemia are strongly associated with a complex aberrant karyotype. Leukemia 2008;22:1539–41.
[4] Kita-Sasai Y, Horiike S, Misawa S, Kaneko H, Kobayashi M, Nakao M, et al. International prognostic scoring system and TP53 mutations are independent prognostic indicators for patients with myelodysplastic syndrome. Br J Haematol 2001;115:309–12.
[5] Seifert H, Mohr B, Thiede C, Oelschlägel U, Schäkel U, Illmer T, et al. Study Alliance Leukemia (SAL). The prognostic impact of 17p (p53) deletion in 2272 adults with acute myeloid leukemia. Leukemia 2009;23:656–63.
[6] Felix CA, Hosler MR, Provisor D, Salhany K, Sexsmith EA, Slater DJ, et al. The p53 gene in pediatric therapy-related leukemia and myelodysplasia. Blood 1996;87:4376–81.
[7] Silveira CG, Oliveira FM, Valera ET, Ikoma MR, Borgonovo T, Cavalli IJ, et al. New recurrent deletions in the PPARgamma and TP53 genes are associated with childhood myelodysplastic syndrome. Leukemia Res 2009;33:19–27.
[8] Koike K, Matsuda K. Recent advances in the pathogenesis and management of juvenile myelomonocytic leukaemia. Br J Haematol 2008;141:567–75.
[9] Loh ML, Sakai DS, Flotho C, Kang M, Fliegauf M, Archambeault S, et al. Mutations in CBL occur frequently in juvenile myelomonocytic leukemia. Blood 2009;114:1859–63.
[10] Sugimoto Y, Muramatsu H, Makishima H, Prince C, Jankowska AM, Yoshida N, et al. Spectrum of molecular defects in juvenile myelomonocytic leukaemia includes ASXL1 mutations. Br J Haematol 2010;150:83–7.
[11] Swerdlow S, Campo E, Lee Harris N, Jaffe E, Pileri S, Stein H, et al. WHO classification of tumours of haematopoietic and lymphoid tissues. 4th ed. IARC Press; 2008.
[12] Matsuda K, Matsuzaki S, Miki J, Hidaka E, Yanagisawa R, Nakazawa Y, et al. Chromosomal change during 6-mercaptopurine (6-MP) therapy in juvenile myelomonocytic leukemia: the growth of a 6-MP-refractory clone that already exists at onset. Leukemia 2006;20:485–90.

Please cite this article in press as: Saito S, et al. Genetic analysis of *TP53* in childhood myelodysplastic syndrome and juvenile myelomonocytic leukemia. Leuk Res (2011), doi:10.1016/j.leukres.2011.06.027

[13] Mitani K, Hangaishi A, Imamura N, Miyagawa K, Ogawa S, Kanda Y, et al. No concomitant occurence of the N-ras and p53 gene mutations in myelodyplastic syndromes. Leukemia 1997;11:863–5.
[14] Tartaglia M, Martinelli S, Cazzaniga G, Cordeddu V, Iavarone I, Spinelli M, et al. Genetic evidence for lineage-related and differentiation stage-related contribution of somatic PTPN11 mutations to leukemogenesis in childhood acute leukemia. Blood 2004;104:307–13.
[15] Kosaki K, Suzuki T, Muroya K, Hasegawa T, Sato S, Matsuo N, et al. PTPN11 (protein-tyrosine phosphatase, nonreceptor-type 11) mutations in seven Japanese patients with Noonan syndrome. J Clin Endocrinol Metab 2002;87:3529–33.
[16] Kiyoi H, Naoe T, Nakano Y, Yokota S, Minami S, Miyawaki S, et al. Prognostic implication of FLT3 and N-RAS gene mutations in acute myeloid leukemia. Blood 1999;93:3074–80.
[17] Spritz RA, Giebel LB, Holmes SA. Dominant negative and loss of function mutations of the c-kit (mast/stem cell growth factor receptor) proto-oncogene in human piebaldism. Am J Hum Genet 1992;50: 261–9.
[18] Jekic B, Novakovic I, Lukovic L, Kuzmanovic M, Popovic B, Milasin J, et al. Lack of TP53 and FMS gene mutations in children with myelodysplastic syndrome. Cancer Genet Cytogenet 2006;166:163–5.
[19] Narumi Y, Aoki Y, Niihori T, Neri G, Cavé H, Verloes A, et al. Molecular and clinical characterization of cardio-facio-cutaneous (CFC) syndrome: overlapping clinical manifestations with Costello syndrome. Am J Med Genet A 2007;143A:799–807.
[20] Kosmider O, Gelsi-Boyer V, Slama L, Dreyfus F, Beyne-Rauzy O, Quesnel B, et al. Mutations of IDH1 and IDH2 genes in early and accelerated phases of myelodysplastic syndromes and MDS/myeloproliferative neoplasms. Leukemia 2010;24:1094–6.
[21] Kobayashi N, Matsuda K, Sakashita K, Matsuzaki S, Iwasaki R, Koike K. Bilineage acute leukemia of T-lymphoid and myeloid lineages. Haematologica 2004;89:1139–41.
[22] Hidaka E, Tanaka M, Matsuda K, Ishikawa-Matsumura M, Yamauchi K, Sano K, et al. A complex karyotype, including a three-way translocation generating a NUP98-HOXD13 transcript, in an infant with acute myeloid leukemia. Cancer Genet Cytogenet 2007;176:137–43.
[23] Andersen MK, Christiansen DH, Kirchhoff M, Pedersen-Bjergaard J. Duplication or amplification of chromosome band 11q23, including the unrearranged MLL gene, is a recurrent abnormality in therapy-related MDS and AML, and is closely related to mutation of the TP53 gene and to previous therapy with alkylating agents. Genes Chromosomes Cancer 2001;31:33–41.
[24] Tauscher M, Göhring G, Glaser S, Hofmann W, Feurstein S, Flotho C, et al. Clonal heterogeneity in childhood myelodysplastic syndromes—challenge for the detection of chromosomal imbalances by array-CGH. Genes Chromosomes Cancer 2010;49:885–900.
[25] De Filippi P, Zecca M, Lisini D, Rosti V, Cagioni C, Carlo-Stella C, et al. Germ-line mutation of the NRAS gene may be responsible for the development of juvenile myelomonocytic leukaemia. Br J Haematol 2009;147:706–9.
[26] Niemeyer CM, Kang MW, Shin DH, Furlan I, Erlacher M, Bunin NJ, et al. Germline CBL mutations cause developmental abnormalities and predispose to juvenile myelomonocytic leukemia. Nat Genet 2010;42:794–800.
[27] Christiansen DH, Andersen MK, Pedersen-Bjergaard J. Mutations with loss of heterozygosity of p53 are common in therapy-related myelodysplasia and acute myeloid leukemia after exposure to alkylating agents and significantly associated with deletion or loss of 5q, a complex karyotype, and a poor prognosis. J Clin Oncol 2001;19:1405–13.
[28] Castro PD, Liang JC, Nagarajan L. Deletions of chromosome 5q13.3 and 17p loci cooperate in myeloid neoplasms. Blood 2000;95:2138–43.

Please cite this article in press as: Saito S, et al. Genetic analysis of *TP53* in childhood myelodysplastic syndrome and juvenile myelomonocytic leukemia. Leuk Res (2011), doi:10.1016/j.leukres.2011.06.027

Journal of Cellular Physiology

Neutrophil Differentiation From Human-Induced Pluripotent Stem Cells

TATSUYA MORISHIMA,[1] KEN-ICHIRO WATANABE,[1] AKIRA NIWA,[2] HISANORI FUJINO,[1] HIROSHI MATSUBARA,[1] SOUICHI ADACHI,[1] HIROFUMI SUEMORI,[3] TATSUTOSHI NAKAHATA,[2] AND TOSHIO HEIKE[1]*

[1]*Department of Pediatrics, Graduate School of Medicine, Kyoto University, Kyoto, Japan*

[2]*Department of Clinical Application, Center for iPS Cell Research and Application, Kyoto University, Kyoto, Japan*

[3]*Laboratory of Embryonic Stem Cell Research, Stem Cell Research Center, Institute for Frontier Medical Sciences, Kyoto University, Kyoto, Japan*

Induced pluripotent stem (iPS) cells are of potential value not only for regenerative medicine, but also for disease investigation. The present study describes the development of a neutrophil differentiation system from human iPS cells (hiPSCs) and the analysis of neutrophil function and differentiation. The culture system used consisted of the transfer of hiPSCs onto OP9 cells and their culture with vascular endothelial growth factor (VEGF). After 10 days, TRA 1-85^{+}CD34^{+}VEGF receptor-2 (VEGFR-2)^{high} cells were sorted and co-cultured with OP9 cells in the presence of hematopoietic cytokines for 30 days. Floating cells were collected and subjected to morphological and functional analysis. These hiPSC-derived neutrophils were similar to peripheral blood mature neutrophils in morphology, contained functional neutrophil specific granules, and were equipped with the basic functions such as phagocytosis, superoxide production, and chemotaxis. In the process of differentiation, myeloid cells appeared sequentially from immature myeloblasts to mature segmented neutrophils. Expression patterns of surface antigen, transcription factors, and granule proteins during differentiation were also similar to those of granulopoiesis in normal bone marrow. In conclusion, differentiation of mature neutrophils from hiPSCs was successfully induced in a similar process to normal granulopoiesis using an OP9 co-culture system. This system may be applied to elucidate the pathogenesis of various hematological diseases that affect neutrophils.

J. Cell. Physiol. 226: 1283–1291, 2011.

Neutrophils and/or myeloid differentiation are most commonly affected in various hematological diseases including inherited bone marrow failure syndromes and neutrophil function disorders. Responsible genes have been identified in most of these syndromes or diseases, but the association between the gene mutation and the specific phenotype is not always clear. Moreover, often patients who present with a specific syndrome lack mutations in the known genes (Alter, 2007). Understanding the pathophysiology of these syndromes has been challenging despite the information provided by recent molecular findings, and in many of these syndromes, experimental models have not yet been generated.

Murine models of human congenital and acquired diseases are invaluable for disease investigation, but they provide a limited representation of human pathophysiology because they often do not faithfully mimic human diseases. The differences between murine and human physiologies make human cell culture an essential complement to research with animal models of disease.

Induced pluripotent stem (iPS) cells are reprogrammed somatic cells with embryonic stem (ES) cell-like characteristics generated by the introduction of combinations of specific transcription factors (Takahashi and Yamanaka, 2006; Meissner et al., 2007; Okita et al., 2007; Takahashi et al., 2007; Yu et al., 2007; Park et al., 2008b). Given the robustness of the approach, direct reprogramming promises to be a facile source of patient-derived cell lines. Such lines would be immediately valuable not only for regenerative medicine, but for disease investigation and drug screening as well.

The pluripotency and self-renewal potential of ES cells contributes to their value in various fields of science (Evans and Kaufman, 1981). Previous studies using normal or gene-manipulated ES cells have helped elucidate the process of normal embryogenesis and the genetic mechanisms of certain diseases (Lensch and Daley, 2006; Tulpule et al., 2010). Use of human embryos, however, faces ethical controversies that hinder the applications of human ES cells (hESCs). In addition, it is difficult to generate patient- or disease-specific ES cells, which are required for their effective application. The use of iPS cells would avoid the controversies surrounding human embryonic stem cell research.

Patient-specific iPS cells can be used for the generation of disease-corrected, patient-specific cells for cell therapy applications. Disease-specific pluripotent cells capable of differentiation into the various tissues affected in each condition can also provide new insights into disease pathophysiology by permitting analysis in a human system, under controlled conditions in vitro. Recent studies reported the generation of disease-specific iPS cell lines from patients with a variety of diseases (Park et al., 2008a; Raya et al., 2009; Agarwal et al., 2010). Therefore, disease-specific iPS cells are expected to be good models for the investigation of different diseases, and

Contract grant sponsor: The Ministry of Education, Culture, Sports, Science and Technology, Japan.

*Correspondence to: Toshio Heike, Department of Pediatrics, Graduate School of Medicine, Kyoto University, 54 Kawahara-cho, Shogoin, Sakyo-ku, Kyoto 606-8507, Japan.
E-mail: heike@kuhp.kyoto-u.ac.jp

Received 21 May 2010; Accepted 20 September 2010

Published online in Wiley Online Library (wileyonlinelibrary.com), 13 October 2010.
DOI: 10.1002/jcp.22456

effective neutrophil differentiation systems are required to investigate the pathogenesis of various hematological conditions that affect neutrophils using human iPS cells (hiPSCs).

Recent reports describe in vitro culture systems for neutrophil differentiation from hESCs (Choi et al., 2009; Saeki et al., 2009; Yokoyama et al., 2009); however, neutrophil differentiation from hiPSCs has not yet been reported in detail. One of these studies demonstrated that myeloid differentiation could be induced from hiPSCs using the same methodology employed for their differentiation from hESCs (Choi et al., 2009), but the differentiation process and the functions of hiPSC-derived neutrophils were not shown in detail. A system for erythroid differentiation from primate ES and murine iPS cells by co-culture with OP9 stromal cells was developed in previous studies (Umeda et al., 2004; Umeda et al., 2006; Shinoda et al., 2007; Niwa et al., 2009). In the present study, a neutrophil differentiation system from hiPSCs was established by modifying the erythroid differentiation system, and the functions of the hiPSC-derived neutrophils and their differentiation process were analyzed in detail. This system may contribute to the elucidation of the pathogenesis of various blood diseases and the development of novel therapeutic approaches.

Materials and Methods

Maintenance of cells

The human iPS cell lines 201B6, 253G1 and 253G4 were a kind gift from Dr. Yamanaka (Kyoto University, Kyoto), and were generated from human dermal fibroblasts by retrovirus-mediated transfection of four (201B6) or three (253G1 and 253G4) transcription factors (Oct3/4, Sox2, and Klf4, with or without c-Myc) (Takahashi et al., 2007; Nakagawa et al., 2008). The human iPS cell lines and the human ES cell line KhES3-EGFPneo (KhES-3G) were maintained on mitomycin-C (Kyowa Hakko Kirin, Tokyo, Japan) -treated mouse embryonic fibroblasts (MEFs) in DMEM/F12 (Sigma-Aldrich, St. Louis, MO) supplemented with 20% Knockout™ Serum Replacement (Invitrogen, Carlsbad, CA), 5 ng/ml basic fibroblast growth factor (bFGF; R&D Systems, Minneapolis, MN), 1% non-essential amino acids solution (Invitrogen), 5 mM sodium hydroxide solution, 100 μM 2-mercaptethanol, and 2 mM L-glutamine. The culture medium was replaced daily with fresh medium. Colonies were passaged onto new MEFs every 3 or 4 days. The human ES cell line was used in conformity with The Guidelines for Derivation and Utilization of Human Embryonic Stem Cells of the Ministry of Education, Culture, Sports, Science, and Technology, Japan. OP9 stromal cells, which were a kind gift from Dr. Kodama (Osaka University, Osaka), were maintained in α-MEM (Invitrogen) supplemented with 20% fetal calf serum (FCS; Biological Industries, Bet Haemek, Israel).

Antibodies

The antibodies used for flow cytometric analysis included fluorescein isothiocyanate (FITC)-conjugated anti-human TRA 1-85 (R&D Systems), CD45 (Becton-Dickinson, Franklin Lakes, NJ) antibodies, phycoerythrin (PE)-conjugated anti-human CD11b, CD34 (Beckman Coulter, Fullerton, CA), CD13, CD16, CD33 (Becton-Dickinson) antibodies, and allophycocyanin (APC)-conjugated anti-human vascular endothelial growth factor receptor-2 (VEGFR-2) (eBioscience, San Diego, CA) antibody. The primary antibodies used for immunocytochemical analysis included goat anti-human lactoferrin (Santa Cruz Biotechnology, Santa Cruz, CA) and rabbit anti-human MMP9 (Abcam, Cambridge, UK). Biotinylated horse anti-goat or anti-rabbit antibodies (Vector Laboratories, Burlingame, CA) were used as secondary antibodies.

Differentiation of iPS cells

Methods used for the initial differentiation of iPS cells and cell sorting were based on earlier reports (Umeda et al., 2004, 2006). Briefly, trypsin-treated undifferentiated iPS cells were transferred onto OP9 cells and cultured with 20 ng/ml vascular endothelial growth factor (VEGF) (R&D Systems). After 10 days, the induced cells were harvested with cell dissociation buffer (Invitrogen), and sorted TRA 1-85^{+}CD34^{+}VEGFR-2^{high} cells were transferred onto fresh OP9 cells in six-well plates at a concentration of 3×10^3 cells per well. Sorted cells were cultured in α-MEM (Invitrogen) containing 10% FCS (Sigma, St Louis, MO), 50 μM 2-mercaptoethanol, 20 ng/ml interleukin (IL)-3, 100 ng/ml stem cell factor (SCF) (R&D Systems), and 10 ng/ml thrombopoietin (TPO) for 20 days. On day 20 after cell sorting, cytokines were changed into 20 ng/ml IL-3 and 10 ng/ml granulocyte colony-stimulating factor (G-CSF). IL-3, TPO and G-CSF were kindly provided by Kyowa Hakko Kirin.

Flow cytometric analysis and cell sorting

Cells were trypsinized and stained with antibodies. Dead cells were excluded by 4',6-diamidino-2-phenylindole (DAPI) staining. Samples were analyzed using an LSR flow cytometer and Cell Quest software (Becton Dickinson). Cell sorting was performed using a FACSVantage SE flow cytometer (Becton Dickinson).

Cytostaining

Floating cells were centrifuged onto glass slides using a Shandon Cytospin® 4 Cytocentrifuge (Thermo, Pittsburgh, PA), and analyzed by microscopy after May–Giemsa, myeloperoxidase (MPO), or alkaline-phosphatase staining. Sequential morphological analysis was performed as follows: all adherent cells including OP9 cells were trypsinized, harvested, and incubated in a new tissue-culture dish (Becton-Dickinson) for 1 h to eliminate adherent OP9 cells (Suwabe et al., 1998). Floating cells were then collected, centrifuged onto glass slides, and analyzed by microscopy after May–Giemsa staining. For immunocytochemical analysis, cells were fixed with 4% paraformaldehyde (PFA), immersed in citrate buffer, and autoclaved for 5 min at 121°C for antigen retrieval (Toda et al., 1999). The slides were then incubated with primary antibodies followed by application of the streptavidinbiotin complex immunoperoxidase technique with diaminobenzidine as chromogen, and nuclei were counterstained with hematoxylin.

Electron microscopy

Cells were fixed in 2% glutaraldehyde in 0.1 M phosphate buffer (PB) for at least 2 h, and then postfixed in 1% osmium tetroxide in 0.1 M PB for 1.5 h. After fixation, samples were dehydrated in a graded ethanol series, cleared with propylene oxide, and embedded in Epon. Thin sections of cured samples were stained with uranyl acetate and Reynolds lead citrate. The sections were inspected using a transmission electron microscope, H7650 (Hitachi, Tokyo, Japan).

Chemotaxis assay

Chemotactic ability was determined using a modified Boyden chamber method (Boyden, 1962; Harvath et al., 1980). Briefly, 500 μl of the reaction medium (Hank's Balanced Salt Solution (HBSS) containing 2.5% FCS) with or without 10 nM formyl-Met-Leu-Phe (fMLP; Sigma-Aldrich) was placed into each well of a 24-well plate, and the cell culture insert (3.0-μm pores; Becton Dickinson) was gently placed into each well to divide the well into upper and lower sections. Floating cells were suspended in the reaction medium at 7.0×10^4/ml, and a 500-μl cell suspension was added to the upper well, allowing the cells to migrate from the upper to the lower side of the membrane for 4 h at 37°C. After incubation, cells in the lower chamber were collected and counted using an LSR flow cytometer. Cells were counted by flow cytometry as follows:

equivalent amounts of counting beads were added to each sample and counted until the bead count reached 10,000.

MPO activity assay

The EnzChek Myeloperoxidase (MPO) Activity Assay Kit (Molecular Probes, Leiden, The Netherlands) was used for rapid and sensitive determination of MPO chlorination activity in cell lysates. The procedure was performed following the manufacturer's instructions. Cell lysate samples were prepared from 1×10^4 floating cells by freeze-thaw cycles. Fluorescence was measured with a fluorescence microplate reader (Wallac 1420 ARVO sx; PerkinElmer, Waltham, MA) using fluorescence excitation and emission at 485 and 530 nm, respectively. The background fluorescence measured for each zero-MPO control reaction was subtracted from each fluorescence measurement before plotting.

DHR assay

Neutrophil production of reactive oxygen species was detected by flow cytometry using dihydrorhodamine123 (DHR) as described previously (Vowells et al., 1995). Briefly, 3.5×10^4 floating cells were suspended in 100 μl of the reaction buffer (HBSS containing 0.1% FCS and 5 mM glucose) per tube, and two tubes were prepared for each sample. Catalase (Sigma-Aldrich) at a final concentration of 1000 U/ml and DHR at a final concentration of 1.0×10^5 nM were added and incubated for 5 min in a 37°C shaking water bath. After incubation, phorbol myristate acetate (PMA; Sigma-Aldrich) at a final concentration of 400 ng/ml was added to one of the two tubes and tubes were returned to the water bath for an additional 15 min. Following incubation, rhodamine fluorescence from the oxidized DHR was detected using an LSR flow cytometer.

Phagocytosis and detection of reactive oxygen species

Phagocytosis and neutrophil production of reactive oxygen species was detected by chemiluminescent microspheres (luminol-binding carboxyl hydrophilic microspheres; TORAY, Tokyo, Japan) as described previously (Uchida et al., 1985). Briefly, 2×10^4 floating cells were suspended in 50 μl of the reaction buffer (HBSS containing 20 mM N-2-hydroxyethylpiperazine-N′-2-ethanesulfonic acid (HEPES)) per tube. To activate the system, 5 μl of chemiluminescent microspheres was added, and light emission was recorded continuously. During the measurement, samples were kept at 37°C. To inhibit the phagocytosis, 1.75 μg of cytochalasin B (Sigma-Aldrich) was added to the sample. Chemiluminescence from the microspheres was detected using a luminometer (TD-20/20; Turner Designs, Sunnyvale, CA).

RNA extraction and RT-PCR analysis

RNA samples were prepared using silica gel membrane-based spin-columns (RNeasy Mini-Kit™, Qiagen, Valencia, CA) and subjected to reverse transcription (RT) with the Ominscript-RT Kit™ (Qiagen). All procedures were performed following the manufacturer's instructions. For reverse transcriptase-polymerase chain reaction (RT-PCR), yields were adjusted by dilution to produce equal amounts of the human glyceraldehyde-3-phosphate dehydrogenase (GAPDH) amplicon. The complementary DNA (cDNA) templates were initially denatured at 94°C for 5 min, followed by 30–40 amplification reactions consisting of 94°C for 15–30 sec (denaturing), 55–63°C for 15–30 sec (annealing), and 72°C for 30–60 sec (extension), with a final extension at 72°C for 7 min. The oligonucleotide primers were as follows: NANOG, 5′-CAG CCC TGA TTC TTC CAC CAG TCC C-3′ and 5′-TGG AAG GTT CCC AGT CGG GTT CAC C-3′ (Takahashi et al., 2007); human GAPDH, 5′-CAC CAG GGC TGC TTT TAA CTC TG-3′ and 5′-ATG GTT CAC ACC CAT GAC GAA C-3′ (Umeda et al., 2006); PU.1, 5′-CTG CAT TGG CCC CCA CCG AG-3′ and 5′-AGG TCT TCT GAT GGC TGA GGG GG-3′; C/EBPα, 5′-TAA CCT TGT GCC TTG GAA ATG CAA AC-3′ and 5′- ATG TTT CCA CCC CTT TCT AAG GAC A-3′ (Duan and Horwitz, 2003); C/EBPε, 5′- AGT CTG GGG AAG AGC AGC TTC-3′ and 5′- ACA GTG TGC CAC TTG GTA CTG-3′ (Mori et al., 2009); MPO, 5′-TGA GGA CGG CTT CTC TCT TC-3′ and 5′-CCC GGT AAG TGA TGA TCT GG-3′; Lactoferrin, 5′-AGC TGG CAG ACT TTG CGC T-3′ and 5′-TTC AGA TTA GTA ATG CCT GCG ACA TAC-3′ (Kholodnyuk et al., 2006); Gelatinase (MMP-9), 5′-GCC TCC AAC CAC CAC CAC AC-3′ and 5′-GCC CAG CCC ACC TCC ACT C-3′ (Sugimoto et al., 2001); mouse GAPDH, 5′-ACG GCC GCA TCT TCT TGT GCA-3′ and 5′-CAC CCT TCA AGT GGG CCC CG-3′. PCR amplification reaction cycles were performed in the linear range for each primer by carrying out primer titrations. The number of reaction cycles per sample were: NANOG, 35 cycles; human GAPDH, 30 cycles; PU.1, 40 cycles; C/EBPα, 40 cycles; C/EBPε, 40 cycles; MPO, 35 cycles; Lactoferrin, 35 cycles; Gelatinase (MMP-9), 40 cycles; mouse GAPDH, 30 cycles.

Statistics

Statistical analyses were conducted using the Student's *t*-test. Statistical significance was defined as $P < 0.05$.

Results

Neutrophil differentiation from hiPSCs in co-culture with OP9 stromal cells

A culture system for the induction of erythroid cell differentiation from primate ES and murine iPS cells by co-culture with OP9 stromal cells (Umeda et al., 2004; Umeda et al., 2006; Shinoda et al., 2007; Niwa et al., 2009) was established, and this system was applied for neutrophil differentiation from hiPSCs. Prior data in primate ES cells suggested that the VEGFR-2^{high} fraction of differentiated cells contained hemangioblasts and VEGFR-2^{high}CD34$^+$ cells had more hematopoietic potential (Umeda et al., 2006). Therefore, the expression of VEGFR-2 and CD34 was examined using three human iPS cell lines (201B6, 253G1, 253G4) and one ES cell line (KhES-3G). After 10 days of co-culture with OP9 in the presence of 20 ng/ml VEGF, VEGFR-2^{high}CD34$^+$ cells appeared from all hiPSC lines in a similar manner to the ES cell line (Fig. 1A). Among these three human iPS cell lines, the highest percentage of VEGFR-2^{high}CD34$^+$ cells was detected in 253G4 (Fig. 1B), and the data on this cell line is therefore presented below.

The VEGFR-2^{high}CD34$^+$ cell fraction was sorted (Fig. 1C) and 1.1×10^4 (range; 0.6–2.2×10^4 in 14 independent cultures) VEGFR-2^{high}CD34$^+$ cells were grown in one 10-cm dish containing hiPSCs. They were then transferred onto fresh OP9 cells and cultured in the presence of hematopoietic cytokines. Around 10 days after cell sorting (day10 + 10), small, round cell colonies appeared (Fig. 1D), and these colonies gradually grew in both size and number (Fig. 1E). At the same time, floating cells also appeared, and the average number of floating cells from 1×10^4 sorted VEGFR-2^{high}CD34$^+$ cells at 30 days after cell sorting (day10 + 30) was 4.1×10^4 (range; 0.2–9.9×10^4 in 11 independent cultures).

May–Giemsa staining of the floating cells on day 10 + 30 revealed that 38.0 ± 1.6% of the cells were stab and segmented neutrophils (Fig. 1F), which were positive for MPO (Fig. 1G) and neutrophil alkaline-phosphatase (Fig. 1H). The rest were mainly immature myeloid cells and a small number of macrophages, and cells of other lineages, such as erythroid or lymphoid cells, were not observed. The frequency of MPO- and neutrophil alkaline-phosphatase-positive cells is shown in Table 1. The results were consistent with the morphological features revealed by May–Giemsa staining.

Surface marker analysis revealed that these floating cells were positive for CD45 and CD11b, and partially positive for CD13, CD33, and CD16 (Fig. 1I). The expression pattern of these surface markers was similar to that of neutrophils or immature myeloid cells in healthy bone marrow (van Lochem et al., 2004), although the CD16 expression level was lower.

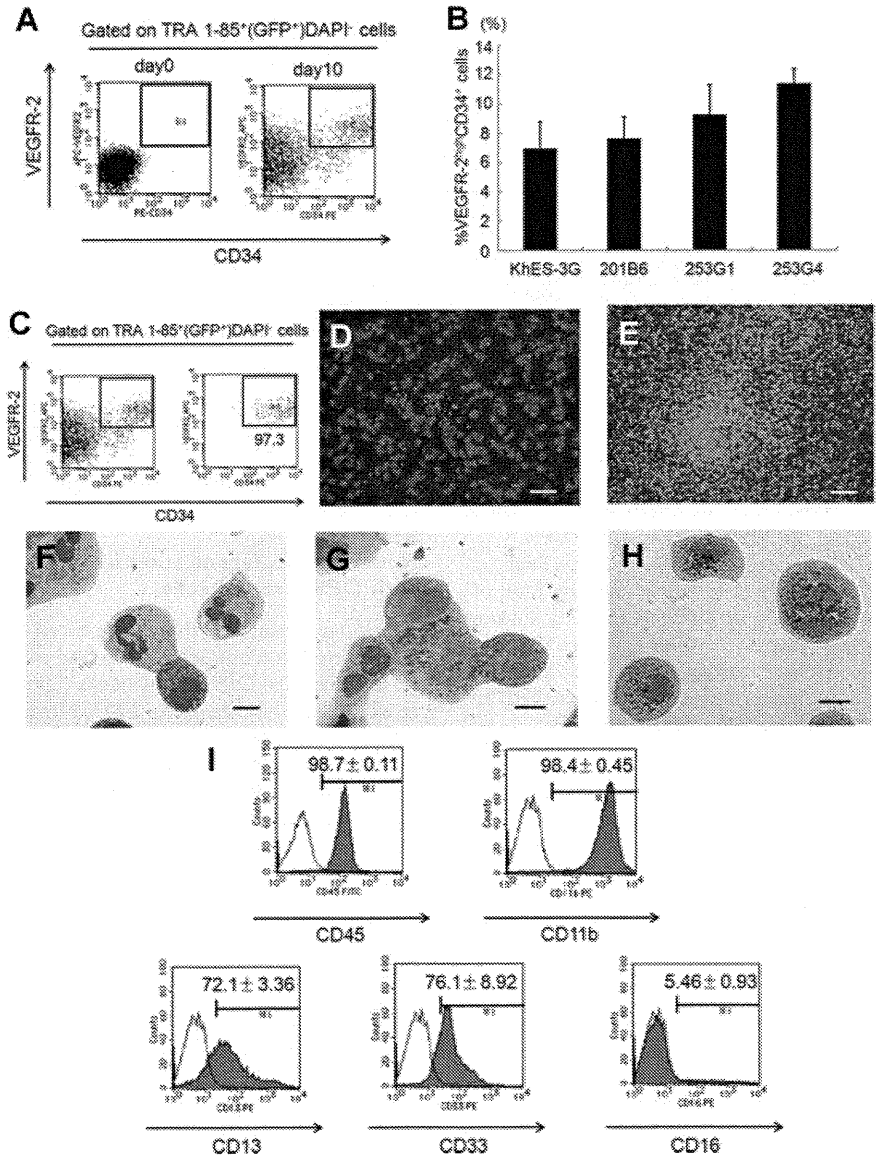

Fig. 1. Neutrophil differentiation from hiPSCs in co-culture with OP9 stromal cells. (A–B) Flow cytometric analysis of VEGFR-2 and CD34 during differentiation induction. TRA 1-85$^+$ (GFP$^+$) DAPI$^-$ cells were gated as human iPS (ES) cell-derived viable cells. Undifferentiated iPS (ES) cells and 10-day culture cells were stained with antibodies specific for VEGFR-2 and CD34. Representative results from one of three independent experiments (A) and percentages of VEGFR-2^{high}CD34$^+$ cells on day 10 (B) are shown (n = 3; bars represent SDs). (C) VEGFR-2^{high}CD34$^+$ cells were sorted on day 10. Representative dot plots and percentages of gated cells are shown. Purities of viable VEGFR-2^{high}CD34$^+$ cells were calculated at 95.5 ± 1.9% from 14 independent experiments. (D–E) Micrographs of adherent hematopoietic cell clusters generated on day 10 (D) and day 30 (E) after cell sorting. Scale bars: 200 μm. (F–H) May–Giemsa staining (F), myeloperoxidase staining (G), and neutrophil alkaline-phosphatase staining (H) of floating cells on day 10 + 30. Scale bars: 10 μm. (I) Flow cytometric analysis of floating cells on day 10 + 30 were stained with antibodies specific for CD45, CD11b, CD13, CD33, or CD16. Plots show the negative control profile (open bars) versus the specific antibody staining profiles (shaded bars). Representative results from one of three independent experiments are shown. [Color figure can be viewed in the online issue, which is available at wileyonlinelibrary.com.]

TABLE 1. Frequency of staining-positive cells for neutrophil specific granules

Staining	Frequency of positive cells (%)
Myeloperoxidase	93.7 ± 1.7
Neutrophil alkaline-phosphatase	39.0 ± 2.2
Lactoferrin	79.0 ± 1.4
Gelatinase	59.0 ± 3.7

Data are shown as mean ± SD (n = 3 independent experiments).

This lower CD16 expression level was similar to that of neutrophils derived in vitro from bone marrow CD34$^+$ cells by stimulation with G-CSF (Kerst et al., 1993b) and to the effect in vivo when G-CSF is administered to healthy volunteers (Kerst et al., 1993a). These results indicated that the modified OP9 co-culture system could differentiate mature neutrophils from immature hiPSCs.

hiPSC-derived neutrophils contain neutrophil specific granules

Mature neutrophils in vivo have intracellular granules that are important for their bactericidal function. The granules can be

classified into three types based on their size, morphology, or electron density, or with reference to a given protein: primary (azurophilic) granules contain MPO, secondary granules contain lactoferrin, and tertiary granules contain gelatinase (Borregaard and Cowland, 1997).

To assess the presence of these granules in hiPSC-derived neutrophils, they were imaged using transmission electron microscopy, which showed that the hiPSC-derived mature neutrophils contained peroxidase-positive and negative granules, as was observed in peripheral blood neutrophils (Fig. 2A–B). Immunocytochemical analysis revealed that hiPSC-derived mature neutrophils were also positive for lactoferrin and gelatinase (Fig. 2C–D). The frequencies of cells that were positive for neutrophil specific granules, as observed by transmission electron microscopy (Table 2) and immunocytochemical analysis (Table 1), were more than 90% for primary granules, about 80% for secondary granules, and approximately 60% for tertiary granules. These results indicated that hiPSC-derived neutrophils contained neutrophils-specific granules.

TABLE 2. Frequency of positive cells for neutrophil specific granules under transmission electron microscopy

Granules	Frequency of positive cells (%)
Peroxidase-positive granules	95.1 (135/142)
Peroxidase-negative granules	86.6 (123/142)

hiPSC-derived neutrophils exhibit biological bactericidal activities

Because neutrophils patrol circulating blood and play a key role in early phase defense mechanisms, the chemotactic, phagocytotic, and bactericidal activities of hiPSC-derived neutrophils were analyzed.

Chemotactic activity was assessed using a modified Boyden chamber method (Boyden, 1962; Harvath et al., 1980). After incubation with or without fMLP in the lower well, neutrophils had migrated from the upper side to the lower side of the membrane. Incubation with fMLP caused an increase in the number of migrated cells of more than three times compared to cells without fMLP, suggesting that hiPSC-derived neutrophils had chemotactic activity in response to a chemoattractant similar to natural neutrophils derived from bone marrow (Fig. 3A).

The MPO-dependent chlorination activity and reactive oxygen production of hiPSC-derived neutrophils, which are both essential for their bactericidal function, were determined next. MPO reacts with hydrogen peroxide (H_2O_2) to form the active redox and enzyme intermediate compound MPO-I, which oxidizes chloride (Cl^-) to HOCl (Winterbourn, 2002). As shown in Figure 3B, hiPSC-derived neutrophils showed MPO-dependent chlorination activity. To evaluate reactive oxygen production, the ability to convert DHR to rhodamine was assessed using flow cytometry (Vowells et al., 1995) and the results revealed that hiPSC-derived neutrophils characteristically produced superoxide in response to PMA (Fig. 3C).

Finally, phagocytotic activity and phagosome-dependent reactive oxygen production were measured using luminol-bound microspheres (Uchida et al., 1985). As shown in Figure 3D, the captured data confirmed that hiPSC-derived neutrophils could produce reactive oxygen species in response to the phagocytosis of microspheres, which was completely abolished in the presence of the antiphagocytic agent cytochalasin B. Moreover, transmission electron microscopy successfully captured a screenshot of a neutrophil phagocytosing the microbeads (Fig. 3E). The above results clearly show that neutrophils derived from hiPSC using the present culture system maintain their functional status.

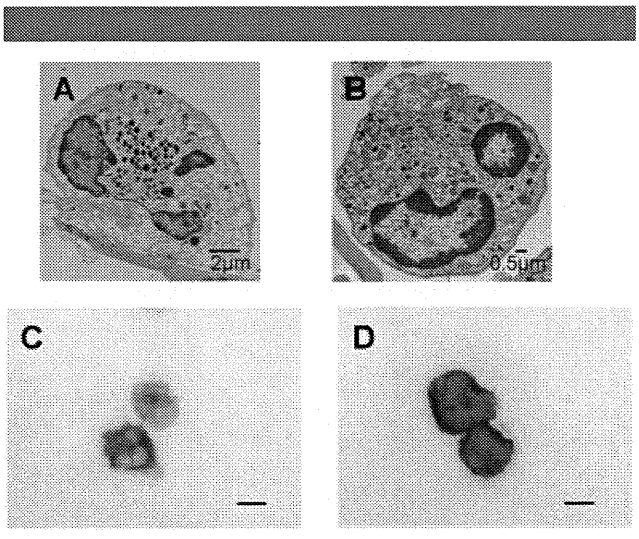

Fig. 2. Neutrophil-specific granules in hiPSC-derived neutrophils. (A–B) Floating cells on day10 + 30 (A) and peripheral blood neutrophils (B) were analyzed by transmission electron microscope. (C–D) Immunocytochemical analysis. Floating cells on day10 + 30 were stained for lactoferrin (C) and MMP9 (gelatinase) (D). Scale bars: 10 μm. [Color figure can be viewed in the online issue, which is available at wileyonlinelibrary.com.]

Step-wise neutrophil differentiation from hiPSCs is similar to normal granulopoiesis

Disorders of neutrophil differentiation are observed in various hematological diseases, among them the maturation arrest of neutrophil precursors in the bone marrow at the promyelocyte stage in severe congenital neutropenia. Thus, in clinical applications for disease investigation, the sequential analysis of the differentiation process from hiPSC to mature neutrophils in this culture system is required.

Observation of the sequential changes in cell morphology was done using May–Giemsa staining. Visualization of the morphology of day10 + 10 cells revealed that the cells were mainly myeloblasts and promyelocytes (Fig. 4A). On day10 + 20, myelocytes and metamyelocytes became predominant (Fig. 4B), and on day 10 + 30, stab and segmented neutrophils became predominant (Fig. 4C).

Surface antigen expression at each differentiation stage of hiPSC-derived cells was analyzed by flow cytometry (Fig. 4D). CD34, cell surface marker on normal immature hematopoietic cells, was detected in about 20% of the cells on day 10 + 10, but disappeared gradually thereafter. From day 10 + 10 to 10 + 30, the common myeloid antigens CD11b and CD33 were expressed in almost all the cells. Interestingly, expression of CD13, also a common myeloid antigen, was observed in less than 20% of cells at day 10 + 10 and did not subsequently increase. The expression level of CD16, which is a representative marker of matured neutrophils (van de Winkel and Anderson, 1991), doubled from day 10 + 10 to day 10 + 20, although the increase in expression was not statistically significant. These expression patterns were consistent with the patterns observed during normal neutrophil differentiation in healthy bone marrow (van Lochem et al., 2004).

The gene expression patterns of the pluripotency marker, transcription factors and granule proteins during neutrophil

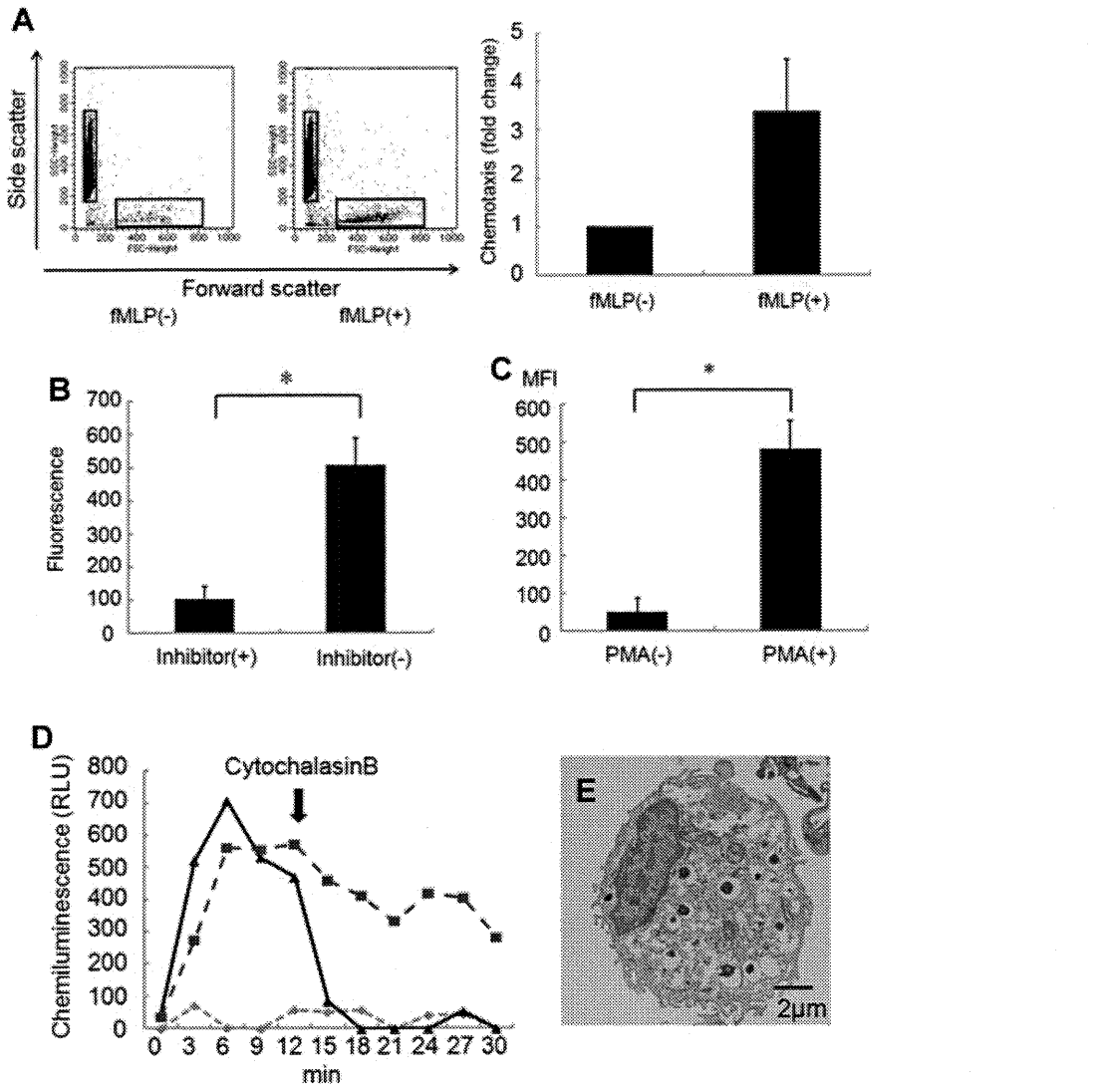

Fig. 3. Functional analysis of hiPSC-derived neutrophils. (A) Chemotactic activity of floating cells on day10 + 30 in response to fMLP was determined as described in Materials and Methods section. After a 4-h culture, the transwell inserts were removed, and the cells in the lower chamber were counted by an LSR flow cytometer (n = 3; bars represent SDs). (B) MPO chlorination activity in cell lysates from floating cells on day10 + 30 was analyzed by EnzChek Myeloperoxidase (MPO) Activity Assay Kit as described in the Materials and Methods section. The chlorination activity in neutrophil cell lysates was almost completely abolished by the addition of a chlorination inhibitor (n = 3; bars represent SDs; *$P < 0.05$.). (C) Floating cells on day10 + 30 were subjected to DHR assay. DHR was reacted with neutrophils with or without PMA, and the resultant rhodamine fluorescence was detected by flow cytometry. The addition of PMA increased the levels of fluorescence. Results are expressed as mean fluorescence intensity (MFI) (n = 3; bars represent SDs; *$P < 0.05$.). (D) Floating cells on day10 + 30 were subjected to the assay for phagocytosis-induced respiratory burst activity using chemiluminescent microspheres (luminol-binding microspheres). Gradual increase in chemiluminescence indicates the respiratory burst triggered by the phagocytosis of luminol-binding microspheres (squares). The increase in chemiluminescence was almost completely abolished by the addition of cytochalasin B (diamonds) and inhibited by its later addition (triangles). The figures are representative of three independent experiments. Abbreviation: RLU, relative light units. (E) hiPSC-derived neutrophils phagocytosing the microbeads were analyzed by transmission electron microscopy.

differentiation in this culture system were investigated by RT-PCR (Fig. 4E–F). NANOG, a pluripotency marker, was expressed in undifferentiated iPS cells but disappeared in sorted VEGFR2^{high}CD34^{+} cells after 10 days differentiation. PU.1 and C/EBPα, essential transcription factors for commitment and differentiation of the granulocytic lineage (Borregaard et al., 2001; Friedman, 2007) were first detected on day 10 + 10 and persisted thereafter. C/EBPε, which had a critical role for the later stages of neutrophil development and transcription of key granule proteins (Borregaard et al., 2001; Friedman, 2007) were first detected faintly on day 10 + 10 and upregulated thereafter. MPO and lactoferrin, which were expressed at the highest levels in myeloblasts/promyelocytes and myelocytes/metamyelocytes, respectively (Cowland and Borregaard, 1999; Borregaard et al., 2001), were detected on day 10 + 10. Gelatinase, which was expressed at the highest level in band and segmented neutrophilic cells (Cowland and Borregaard, 1999; Borregaard et al., 2001), was first detected on day 10 + 20 and upregulated thereafter. Altogether, these results suggested that the neutrophil differentiation in this co-culture system might recapitulate the orderly differentiation process in bone marrow.

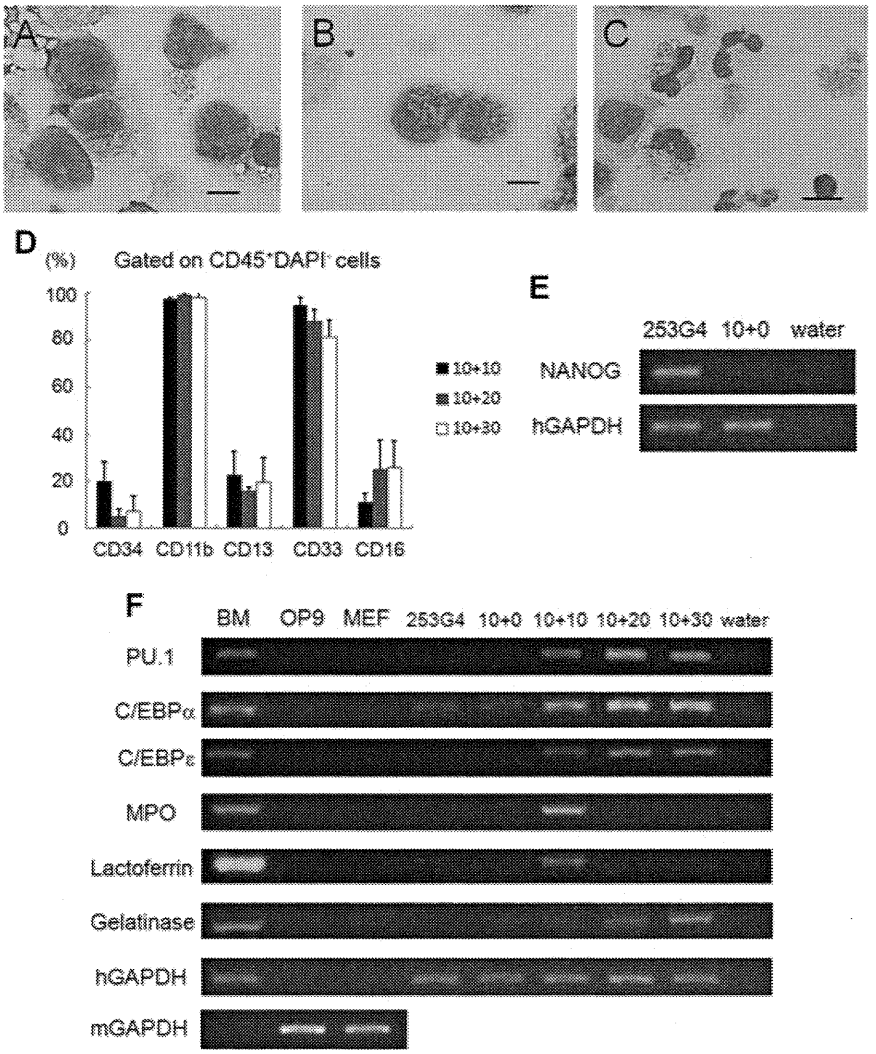

Fig. 4. Sequential analysis of neutrophil differentiation from hiPSCs. (A–C) Sequential morphological analysis of day 10 + 10 (A), day 10 + 20 (B) and day 10 + 30 (C). Scale bars: 10 μm. (D) Surface antigen expression at each level of differentiation of hiPSC-derived cells was analyzed by flow cytometry. All adherent cells including OP9 cells were harvested and stained with antibodies. Human $CD45^{+}DAPI^{-}$ cells were gated as hiPSC-derived viable leukocytes (n = 3; bars represent SDs). (E–F) Sequential RT-PCR analysis of a pluripotency marker (E), genes associated with neutrophil development and neutrophils-specific granules (F) during differentiation. Human GAPDH was used as a loading control. Abbreviations: BM, human bone marrow cells; 253G4, undifferentiated 253G4 cells; 10 + 0, sorted $VEGFR2^{high}CD34^{+}$ cells after 10 days differentiation; 10 + 10, 20, 30, all cells after 10, 20, 30 days differentiation after cell sorting; hGAPDH, human GAPDH; mGAPDH, mouse GAPDH. The figures are representative of three independent experiments. [Color figure can be viewed in the online issue, which is available at wileyonlinelibrary.com.]

Discussion

The analysis of the differentiation process of neutrophils can provide helpful information for the elucidation of the pathogenesis of hematopoietic diseases that affect neutrophils and/or myeloid differentiation, including inherited bone marrow failure syndromes and neutrophil function disorders. Traditionally, HL-60, an acute promyelocytic cell line, has been used as a neutrophil differentiation model (Collins et al., 1978; Newburger et al., 1979). Although this cell line grows well and differentiates easily into neutrophils, the neutrophil differentiation model is not suitable for the analysis of neutrophil-affected disorders because of its leukemic cell-origin. Development of a neutrophil differentiation system based on iPS cells would provide a better model for the analysis of such diseases, because iPS cells can be generated from the somatic cells of patients suffering from these diseases.

The current study aimed to investigate two issues in hiPSC-derived neutrophil differentiation: tracking the step-wise maturation in vitro and evaluating the wide spectrum of neutrophil functions. Through the use of a modified OP9 co-culture system, the directed and step-wise differentiation from hiPSCs to mature neutrophils containing neutrophil specific granules was first accomplished. The expression of surface antigens, transcription factors and granule proteins during differentiation exhibited the characteristic pattern of normal granulopoiesis. The biological functions of hiPSC-derived neutrophils were demonstrated through the quantitative assessment of granule enzyme activities and biological bactericidal activities such as chemotaxis and phagocytosis.

Defects in the maturation and function of neutrophils are associated with certain blood diseases including inherited bone marrow failure syndromes and neutrophil function disorders.

Among bone marrow failure syndromes, certain conditions affect a specific maturation stage, such as the maturation arrest at the plomyelocyte/myelocyte stage seen in severe congenital neutropenia. Neutrophil function disorders can affect specific bactericidal activities, such as the absence of MPO activity characteristic of MPO deficiency disorders. The use of hiPSCs for the investigation of these diseases requires sequential analyses that can identify each neutrophil maturation stage and include a functional analysis to evaluate each bactericidal activity separately on disease-specific, iPSC-derived neutrophils. Although previous studies have reported neutrophil differentiation models from hESCs (Choi et al., 2009; Saeki et al., 2009; Yokoyama et al., 2009) and hiPSC-derived neutrophils have been shown before (Choi et al., 2009), evidence showing that hiPSCs, which are artificially reprogrammed somatic cells, can follow the normal developmental pathway into fully functional mature neutrophils is of great significance, and the description of methods for identifying each neutrophil maturation step and analyzing each bactericidal pathway separately is important for clinical applications.

Although flow-cytometric analysis combined with RT-PCR identified the neutrophil maturation step relatively successfully, discrepancies between the neutrophil differentiation system in this study and normal granulopoiesis were noted such as the lower expression of CD16 than that shown by previous reports on hESC-derived neutrophils (Choi et al., 2009; Saeki et al., 2009; Yokoyama et al., 2009). As CD16 is a mature neutrophil marker in peripheral blood, two reasons could explain this phenomenon. First, residual precursors could have been more significant contaminants in the present system than in previously reported methods due to the function of cytokines and stroma supporting immature hematopoietic cells. Another possible reason is the shift of protein types between membrane-bound and soluble forms. Calluri previously reported that G-CSF is not only a myeloid cell growth factor, but also a modulator of neutrophil behavior (Carulli, 1997), and its stimulation decreases the membrane bound CD16 and increases its soluble form. Low CD16 expression has been documented in neutrophils derived in vitro from bone marrow $CD34^+$ cells by stimulation with G-CSF (Kerst et al., 1993b), and it has been observed in vivo when G-CSF is administered to healthy volunteers (Kerst et al., 1993a). This phenomenon, which is also documented in a report of hESC-derived neutrophils (Yokoyama et al., 2009), is unavoidable in differentiation culture systems using recombinant cytokines. The combination of flow cytometric and PCR analyses enables a more accurate staging of progenitors that could be of importance in the investigation of maturation arrest in future studies.

The culture system presented in this study is considered ineligible for clinical applications due to the use of xenogeneic factors such as OP9 cells and FCS. To overcome this problem, a xeno-free hematopoietic differentiation system from pluripotent cells is currently being established.

In conclusion, the present study shows the establishment of a fully functional mature neutrophil differentiation system from hiPSCs and the detailed analysis of their function and differentiation process. This system could become a useful tool for the investigation of various hematological diseases with defects in maturation and function of neutrophils.

Acknowledgments

We thank Dr. Yamanaka for providing the human iPS cell lines 201B6, 253G1, and 253G4, and Dr. Kodama for providing the OP9 cells. We are grateful to Kyowa Hakko Kirin for providing IL-3, TPO, and G-CSF. We also thank the Center for Anatomical Studies, Kyoto University Graduate School of Medicine for immunocytochemical analysis and transmission electron microscopy analysis. This work was supported by grants from the Ministry of Education, Culture, Sports, Science and Technology, Japan. This work was also supported by the Global COE Program "Center for Frontier Medicine" by the Ministry of Education, Culture, Sports, Science, and Technology (MEXT), Japan.

References

Agarwal S, Loh YH, McLoughlin EM, Huang J, Park IH, Miller JD, Huo H, Okuka M, Dos Reis RM, Loewer S, Ng HH, Keefe DL, Goldman FD, Klingelhutz AJ, Liu L, Daley GQ. 2010. Telomere elongation in induced pluripotent stem cells from dyskeratosis congenita patients. Nature 464:292–296.

Alter BP. 2007. Diagnosis, genetics, and management of inherited bone marrow failure syndromes. Hematology Am Soc Hematol Educ Program 29–39.

Borregaard N, Cowland JB. 1997. Granules of the human neutrophilic polymorphonuclear leukocyte. Blood 89:3503–3521.

Borregaard N, Theilgaard-Monch K, Sorensen OE, Cowland JB. 2001. Regulation of human neutrophil granule protein expression. Curr Opin Hematol 8:23–27.

Boyden S. 1962. The chemotactic effect of mixtures of antibody and antigen on polymorphonuclear leucocytes. J Exp Med 115:453–466.

Carulli G. 1997. Effects of recombinant human granulocyte colony-stimulating factor administration on neutrophil phenotype and functions. Haematologica 82:606–616.

Choi KD, Vodyanik MA, Slukvin II. 2009. Generation of mature human myelomonocytic cells through expansion and differentiation of pluripotent stem cell-derived lin-CD34+CD43+CD45+ progenitors. J Clin Invest 119:2818–2829.

Collins SJ, Ruscetti FW, Gallagher RE, Gallo RC. 1978. Terminal differentiation of human promyelocytic leukemia cells induced by dimethyl sulfoxide and other polar compounds. Proc Natl Acad Sci USA 75:2458–2462.

Cowland JB, Borregaard N. 1999. The individual regulation of granule protein mRNA levels during neutrophil maturation explains the heterogeneity of neutrophil granules. J Leukoc Biol 66:989–995.

Duan Z, Horwitz M. 2003. Targets of the transcriptional repressor oncoprotein Gfi-1. Proc Natl Acad Sci USA 100:5932–5937.

Evans MJ, Kaufman MH. 1981. Establishment in culture of pluripotential cells from mouse embryos. Nature 292:154–156.

Friedman AD. 2007. Transcriptional control of granulocyte and monocyte development. Oncogene 26:6816–6828.

Harvath L, Falk W, Leonard EJ. 1980. Rapid quantitation of neutrophil chemotaxis: use of a polyvinylpyrrolidone-free polycarbonate membrane in a multiwell assembly. J Immunol Methods 37:39–45.

Kerst JM, de Haas M, van der Schoot CE, Slaper-Cortenbach IC, Kleijer M, von dem Borne AE, van Oers RH. 1993a. Recombinant granulocyte colony-stimulating factor administration to healthy volunteers: induction of immunophenotypically and functionally altered neutrophils via an effect on myeloid progenitor cells. Blood 82:3265–3272.

Kerst JM, van de Winkel JG, Evans AH, de Haas M, Slaper-Cortenbach IC, de Wit TP, von dem Borne AE, van der Schoot CE, van Oers RH. 1993b. Granulocyte colony-stimulating factor induces hFc gamma RI (CD64 antigen)-positive neutrophils via an effect on myeloid precursor cells. Blood 81:1457–1464.

Kholodnyuk ID, Kozireva S, Kost-Alimova M, Kashuba V, Klein G, Imreh S. 2006. Down regulation of 3p genes, LTF, SLC38A3 and DRR1, upon growth of human chromosome 3-mouse fibrosarcoma hybrids in severe combined immunodeficiency mice. Int J Cancer 119:99–107.

Lensch MW, Daley GQ. 2006. Scientific and clinical opportunities for modeling blood disorders with embryonic stem cells. Blood 107:2605–2612.

Meissner A, Wernig M, Jaenisch R. 2007. Direct reprogramming of genetically unmodified fibroblasts into pluripotent stem cells. Nat Biotechnol 25:1177–1181.

Mori Y, Iwasaki H, Kohno K, Yoshimoto G, Kikushige Y, Okeda A, Uike N, Niiro H, Takenaka K, Nagafuji K, Miyamoto T, Harada M, Takatsu K, Akashi K. 2009. Identification of the human eosinophil lineage-committed progenitor: revision of phenotypic definition of the human common myeloid progenitor. J Exp Med 206:183–193.

Nakagawa M, Koyanagi M, Tanabe K, Takahashi K, Ichisaka T, Aoi T, Okita K, Mochiduki Y, Takizawa N, Yamanaka S. 2008. Generation of induced pluripotent stem cells without Myc from mouse and human fibroblasts. Nat Biotechnol 26:101–106.

Newburger PE, Chovaniec ME, Greenberger JS, Cohen HJ. 1979. Functional changes in human leukemic cell line HL-60. A model for myeloid differentiation. J Cell Biol 82:315–322.

Niwa A, Umeda K, Chang H, Saito M, Okita K, Takahashi K, Nakagawa M, Yamanaka S, Nakahata T, Heike T. 2009. Orderly hematopoietic development of induced pluripotent stem cells via Flk-1(+) hemoangiogenic progenitors. J Cell Physiol 221:367–377.

Okita K, Ichisaka T, Yamanaka S. 2007. Generation of germline-competent induced pluripotent stem cells. Nature 448:313–317.

Park IH, Arora N, Huo H, Maherali N, Ahfeldt T, Shimamura A, Lensch MW, Cowan C, Hochedlinger K, Daley GQ. 2008a. Disease-specific induced pluripotent stem cells. Cell 134:877–886.

Park IH, Zhao R, West JA, Yabuuchi A, Huo H, Ince TA, Lerou PH, Lensch MW, Daley GQ. 2008b. Reprogramming of human somatic cells to pluripotency with defined factors. Nature 451:141–146.

Raya A, Rodriguez-Piza I, Guenechea G, Vassena R, Navarro S, Barrero MJ, Consiglio A, Castella M, Rio P, Sleep E, Gonzalez F, Tiscornia G, Garreta E, Aasen T, Veiga A, Verma IM, Surralles J, Bueren J, Izpisua Belmonte JC., 2009. Disease-corrected haematopoietic progenitors from Fanconi anaemia induced pluripotent stem cells. Nature 460:53–59.

Saeki K, Nakahara M, Matsuyama S, Nakamura N, Yogiashi Y, Yoneda A, Koyanagi M, Kondo Y, Yuo A. 2009. A feeder-free and efficient production of functional neutrophils from human embryonic stem cells. Stem Cells 27:59–67.

Shinoda G, Umeda K, Heike T, Arai M, Niwa A, Ma F, Suemori H, Luo HY, Chui DH, Torii R, Shibuya M, Nakatsuji N, Nakahata T. 2007. alpha4-Integrin(+) endothelium derived from primate embryonic stem cells generates primitive and definitive hematopoietic cells. Blood 109:2406–2415.

Sugimoto C, Fujieda S, Sunaga H, Noda I, Tanaka N, Kimura Y, Saito H, Matsukawa S. 2001. Granulocyte colony-stimulating factor (G-CSF)-mediated signaling regulates type IV collagenase activity in head and neck cancer cells. Int J Cancer 93:42–46.

Suwabe N, Takahashi S, Nakano T, Yamamoto M. 1998. GATA-1 regulates growth and differentiation of definitive erythroid lineage cells during in vitro ES cell differentiation. Blood 92:4108–4118.

Takahashi K, Tanabe K, Ohnuki M, Narita M, Ichisaka T, Tomoda K, Yamanaka S. 2007. Induction of pluripotent stem cells from adult human fibroblasts by defined factors. Cell 131:861–872.

Takahashi K, Yamanaka S. 2006. Induction of pluripotent stem cells from mouse embryonic and adult fibroblast cultures by defined factors. Cell 126:663–676.

Toda Y, Kono K, Abiru H, Kokuryo K, Endo M, Yaegashi H, Fukumoto M. 1999. Application of tyramide signal amplification system to immunohistochemistry: a potent method to localize antigens that are not detectable by ordinary method. Pathol Int 49:479–483.

Tulpule A, Lensch MW, Miller JD, Austin K, D'Andrea A, Schlaeger TM, Shimamura A, Daley GQ. 2010. Knockdown of Fanconi anemia genes in human embryonic stem cells reveals early developmental defects in the hematopoietic lineage. Blood 115:3453–3462.

Uchida T, Kanno T, Hosaka S. 1985. Direct measurement of phagosomal reactive oxygen by luminol-binding microspheres. J Immunol Methods 77:55–61.

Umeda K, Heike T, Yoshimoto M, Shinoda G, Shiota M, Suemori H, Luo HY, Chui DH, Torii R, Shibuya M, Nakatsuji N, Nakahata T. 2006. Identification and characterization of hemoangiogenic progenitors during cynomolgus monkey embryonic stem cell differentiation. Stem Cells 24:1348–1358.

Umeda K, Heike T, Yoshimoto M, Shiota M, Suemori H, Luo HY, Chui DH, Torii R, Shibuya M, Nakatsuji N, Nakahata T. 2004. Development of primitive and definitive hematopoiesis from nonhuman primate embryonic stem cells in vitro. Development 131:1869–1879.

van de Winkel JG, Anderson CL. 1991. Biology of human immunoglobulin G Fc receptors. J Leukoc Biol 49:511–524.

van Lochem EG, van der Velden VH, Wind HK, te Marvelde JG, Westerdaal NA, van Dongen JJ. 2004. Immunophenotypic differentiation patterns of normal hematopoiesis in human bone marrow: reference patterns for age-related changes and disease-induced shifts. Cytometry B Clin Cytom 60:1–13.

Vowells SJ, Sekhsaria S, Malech HL, Shalit M, Fleisher TA. 1995. Flow cytometric analysis of the granulocyte respiratory burst: a comparison study of fluorescent probes. J Immunol Methods 178:89–97.

Winterbourn CC. 2002. Biological reactivity and biomarkers of the neutrophil oxidant, hypochlorous acid. Toxicology 181-182:223–227.

Yokoyama Y, Suzuki T, Sakata-Yanagimoto M, Kumano K, Higashi K, Takato T, Kurokawa M, Ogawa S, Chiba S. 2009. Derivation of functional mature neutrophils from human embryonic stem cells. Blood 113:6584–6592.

Yu J, Vodyanik MA, Smuga-Otto K, Antosiewicz-Bourget J, Frane JL, Tian S, Nie J, Jonsdottir GA, Ruotti V, Stewart R, Slukvin II, Thomson JA. 2007. Induced pluripotent stem cell lines derived from human somatic cells. Science 318:1917–1920 .

Rapid diagnosis of FHL3 by flow cytometric detection of intraplatelet Munc13-4 protein

Yuuki Murata,[1] Takahiro Yasumi,[1] Ryutaro Shirakawa,[2] Kazushi Izawa,[1] Hidemasa Sakai,[1] Junya Abe,[1] Naoko Tanaka,[1] Tomoki Kawai,[1] Koichi Oshima,[3-5] Megumu Saito,[3] Ryuta Nishikomori,[1] Osamu Ohara,[4,5] Eiichi Ishii,[6] Tatsutoshi Nakahata,[3] Hisanori Horiuchi,[2] and Toshio Heike[1]

[1]Department of Pediatrics, Kyoto University Graduate School of Medicine, Kyoto, Japan; [2]Department of Molecular and Cellular Biology, Institute of Development, Aging and Cancer, Tohoku University, Sendai, Japan; [3]Clinical Application Department, Center for iPS Cell Research and Application, Kyoto University, Kyoto, Japan; [4]Department of Human Genome Research, KAZUSA DNA Research Institute, Kisarazu, Japan; [5]Laboratory for Immunogenomics, Research Center for Allergy and Immunology, RIKEN, Yokohama, Japan; and [6]Department of Pediatrics, Ehime University Graduate School of Medicine, Toon, Japan

Familial hemophagocytic lymphohistiocytosis (FHL) is a potentially lethal genetic disorder of immune dysregulation that requires prompt and accurate diagnosis to initiate life-saving immunosuppressive therapy and to prepare for hematopoietic stem cell transplantation. In the present study, 85 patients with hemophagocytic lymphohistiocytosis were screened for FHL3 by Western blotting using platelets and by natural killer cell lysosomal exocytosis assay. Six of these patients were diagnosed with FHL3. In the acute disease phase requiring platelet transfusion, it was difficult to diagnose FHL3 by Western blot analysis or by lysosomal exocytosis assay. In contrast, the newly established flow cytometric analysis of intraplatelet Munc13-4 protein expression revealed bimodal populations of normal and Munc13-4–deficient platelets. These findings indicate that flow cytometric detection of intraplatelet Munc13-4 protein is a sensitive and reliable method to rapidly screen for FHL3 with a very small amount of whole blood, even in the acute phase of the disease. (*Blood.* 2011;118(5):1225-1230)

Introduction

The granule-dependent cytotoxic pathway is a major immune effector mechanism used by cytotoxic T lymphocytes (CTLs) and natural killer (NK) cells.[1] The pathway involves a series of steps, including cell activation, polarization of the lysosomal granules to the immunologic synapse, exocytosis of lytic proteins such as perforin and granzymes, and induction of apoptosis in the target cells.[2] In addition to its central role in the defense against intracellular infections and in tumor immunity, this pathway also plays an important role in the regulation of immune homeostasis. Defects in the granule-dependent cytotoxic pathway result in a catastrophic hyperinflammatory condition known as hemophagocytic lymphohistiocytosis (HLH).[1,3]

HLH is a life-threatening syndrome of immune dysregulation resulting from the uncontrolled activation and proliferation of CTLs, which leads to macrophage activation and the excessive release of inflammatory cytokines.[4,5] Clinical diagnosis of HLH is made on the basis of cardinal signs and symptoms including prolonged fever and hepatosplenomegaly, and by characteristic laboratory findings such as pancytopenia, hyperferritinemia, hypofibrinogenemia, increased levels of soluble IL-2 receptor, and low or absent NK cell activity.[5,6] HLH can be classified into primary (genetic) or secondary (acquired) forms according to the underlying etiology, although this distinction is difficult to make in clinical practice.[4,5]

Familial hemophagocytic lymphohistiocytosis (FHL) encompasses major forms of primary HLH for which mutations in the genes encoding perforin (*PRF1*; FHL2),[7] Munc13-4 (*UNC13D*; FHL3),[8] syntaxin-11 (*STX11*; FHL4),[9] and syntaxin-binding protein 2 (also known as Munc18-2) (*STXBP2*; FHL5)[10,11] have been identified to date. Perforin is a cytolytic effector that forms a pore-like structure in the target cell membrane. Munc13-4, syntaxin-11, and Munc18-2 are involved in intracellular trafficking or the fusion of cytolytic granules to the plasma membrane and the subsequent delivery of their contents into target cells.[1,12] Consequently, defective cytotoxic activity of CTLs and NK cells is one of the hallmark findings of FHL,[7,8,13-16] although NK cell activity is also decreased in some cases of secondary HLH.[15,17-20]

Prompt and accurate diagnosis of FHL is mandatory to initiate life-saving immunosuppressive therapy and to prepare for hematopoietic stem cell transplantation. Detection of perforin expression in NK cells with flow cytometry is a reliable method to screen for FHL2.[21] Another test analyzes the expression of CD107a on the surface of NK cells, which marks the release of cytolytic granules.[22] Reduced expression of CD107a implies impaired degranulation of NK cells and predicts a likelihood of FHL3.[23] However, this analysis is not available in some patients with extremely reduced NK cell numbers, such as during the acute phase of HLH.[19] In addition, NK-cell degranulation is also impaired in FHL4[24] and FHL5,[10,11] making it impossible to differentiate these disorders.

We reported previously that Munc13-4 protein is expressed in platelets and regulates the secretion of dense core granules.[25] Herein we report that Munc13-4 is expressed far more abundantly in platelets than in PBMCs. We also describe the development of a

Submitted January 10, 2011; accepted May 23, 2011. Prepublished online as *Blood* First Edition paper, June 8, 2011; DOI 10.1182/blood-2011-01-329540.

The online version of this article contains a data supplement.

The publication costs of this article were defrayed in part by page charge payment. Therefore, and solely to indicate this fact, this article is hereby marked "advertisement" in accordance with 18 USC section 1734.

new method to screen for FHL3 rapidly by detecting intraplatelet Munc13-4 expression through flow cytometry.

Methods

Patients

Between January 2008 and March 2010, whole blood samples from 85 patients were screened for FHL3. The patients had been clinically diagnosed with HLH by their referring physicians and were suspected of possible FHL. Characteristics of the enrolled patients are summarized in supplemental Table 1 (available on the *Blood* Web site; see the Supplemental Materials link at the top of the online article). As a control, blood obtained from healthy adults at the time of patient sampling was shipped for screening along with the patient samples. Before the laboratory studies were performed, informed consent was obtained from the patients and their parents, in accordance with the institutional review board of Kyoto University Hospital and the Declaration of Helsinki.

Preparation of PBMCs and platelet samples

Whole blood samples treated with EDTA were centrifuged gently at 100*g* for 10 minutes, and platelets were collected from the supernatant plasma layer. Alternatively, platelets were prepared from small aliquots of blood samples by lysing red blood cells with ammonium chloride. PBMCs were obtained by Ficoll-Hypaque density gradient centrifugation from the remaining sample. $CD4^+$, $CD8^+$, $CD14^+$, $CD19^+$, and $CD45^+$ cells were separated from PBMCs using an AutoMACS Pro (Miltenyi Biotec) and magnetic bead–conjugated mAbs according to the manufacturer's instructions. Flow cytometric analysis revealed that each cell population contained > 95% $CD4^+$, $CD8^+$, $CD14^+$, $CD19^+$, and $CD45^+$ cells (data not shown).

Mutation analysis

Genomic DNA was isolated from the PBMCs of patients with defective Munc13-4 expression using standard procedures. Primers were designed for the amplification and direct DNA sequencing of the *UNC13D*-coding exons, including the adjacent intronic sequences for the identification of splice-site variants. Primer sequences are available upon request. Products were sequenced directly with an ABI3130 genetic analyzer (Applied Biosystems).

Antibodies

Rabbit polyclonal antibodies raised against the N-terminal region (residues 1-262)[25] and full-length human Munc13-4 protein were used as primary antibodies for Western blot and flow cytometric analysis, respectively. Rabbit polyclonal anti-integrin αIIb (Santa Cruz Biotechnology) and mouse polyclonal anti–β-actin (Sigma-Aldrich) antibodies were used as primary antibodies for Western blotting. The mAbs used in the flow cytometric analysis were FITC-conjugated anti-CD3 (SK7; BD Pharmingen), phycoerythrin (PE)–conjugated anti-CD41a (HIP8; BD Pharmingen); allophycocyanin-conjugated anti-CD56 (N901; Beckman Coulter), and PE-conjugated anti-CD107a (H4A3; eBioscience).

Western blot analysis

Cell extracts were fractionated by SDS-PAGE, and the fractionated proteins were electrotransferred onto polyvinylidene fluoride membranes. The membranes were blocked overnight in blocking buffer (5% skim milk) and incubated for 1 hour at room temperature with the primary antibodies, followed by HRP-conjugated anti–rabbit or anti–mouse IgG polyclonal antibodies (Santa Cruz Biotechnology). Specific bands were visualized by the standard enhanced chemiluminescence method.

Flow cytometric analysis of Munc13-4 protein

After surface staining with anti-CD41a mAbs, platelets were fixed and permeabilized by Cytofix/Cytoperm (BD Biosciences) and washed 3 times with Perm/Wash buffer (BD Biosciences). After nonspecific reactions were blocked with Chrome-Pure human IgG (Jackson ImmunoResearch Laboratories), rabbit polyclonal antibody against the full-length human Munc13-4 protein was added, followed by FITC-conjugated donkey anti–rabbit IgG (Jackson ImmunoResearch Laboratories). Platelets were gated on the basis of their appearance on forward- and side-scatter plots in log/log scale and by CD41a expression. The gated platelets were analyzed for Munc13-4 expression by flow cytometry (FACSCalibur; BD Biosciences).

Lysosomal degranulation assays

To quantify lysosome exocytosis by NK cells, 2×10^5 PBMCs were mixed with 2×10^5 human erythroleukemia cell line K562 cells and incubated for 2 hours in complete medium (RPMI 1640 medium supplemented with 2mM L-glutamine and 10% FCS) at 37°C in 5% CO_2. Cells were resuspended in PBS supplemented with 2% FCS and 2mM EDTA; stained with anti-CD3–FITC, anti-CD56–allophycocyanin, and anti-CD107a–PE mAbs; and analyzed by flow cytometry.

Platelet exocytosis of the lysosomal granules was analyzed as described previously[26] but with a minor modification. Briefly, platelets were suspended in PBS containing 2mM EDTA and PE-conjugated anti-CD107a mAb, stimulated with 5 U/mL of thrombin (Wako Pure Chemical Industries) for 10 minutes at 25°C, and immediately analyzed by flow cytometry. The degranulation index of platelets was calculated as: (mean fluorescence value of stimulated sample − mean fluorescence value of nonstimulated sample)/mean fluorescence value of nonstimulated sample.

Statistical analysis

Statistical analyses were performed with 1-way ANOVA followed by the Tukey post hoc test to compare multiple groups, with a $P < .05$ level considered to be significant.

Results

Diagnosis of FHL3 by Western blot analysis using platelets

Before screening for FHL3, the Munc13-4 expression level was compared between platelets and PBMCs. Munc13-4 expression in platelets was approximately 10 times higher than that in PBMCs (Figure 1A). $CD8^+$ cells expressed a similar level of Munc13-4 protein as other PBMC cell types (Figure 1B). Similar amounts of platelet- and PBMC-derived proteins could be obtained from a sample (data not shown). Therefore, platelets were used to perform Western blotting to screen for Munc13-4 deficiency. Of the 85 patients screened, 6 patients were diagnosed with FHL3 (Figure 1C). Munc13-4 protein was barely detected in the platelets of each FHL3 patient regardless of the gene mutation (Table 1). For each sample, no more than 1 mL of whole blood was required to perform the analysis.

Difficulty in diagnosing FHL3 in the acute phase of the disease

Patients in the acute phase of the disease who require screening for FHL often receive platelet transfusions because of thrombocytopenia.[4-6] To study the effect of transfused platelets on screening results, FHL3 screening was attempted in a patient receiving platelet transfusions. As expected, Western blotting using platelets could not detect Munc13-4 deficiency because of the normal expression of the protein in the transfused platelets (Figure 2A left column). Surprisingly, Western blotting using PBMCs also could not clearly identify Munc13-4 deficiency because a substantial number of platelets were present in the PBMCs obtained by the standard method (Figure 2A right column). By positively selecting $CD45^+$ cells and removing platelets, it was found that a considerable amount of the Munc13-4 protein detected in PBMC samples

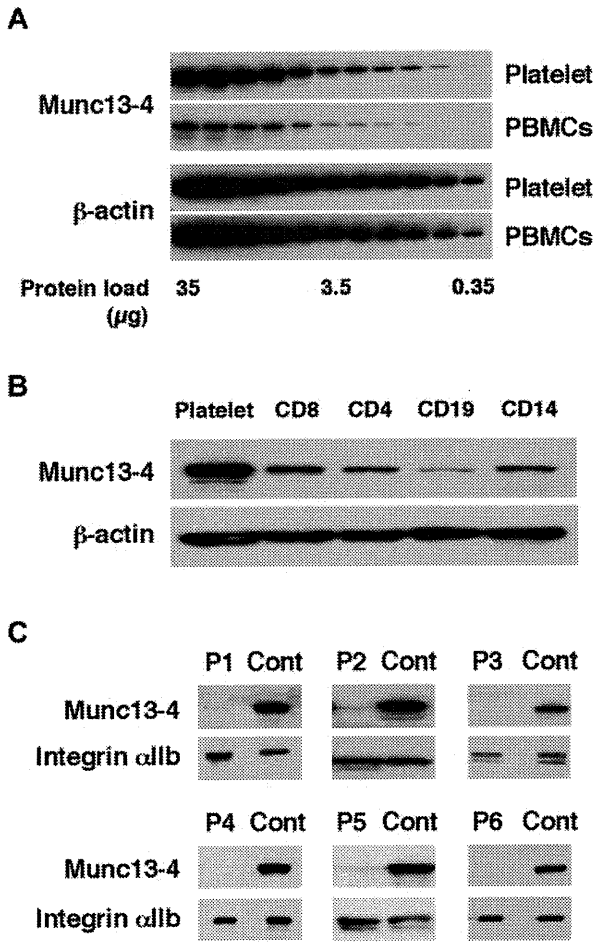

Figure 1. Diagnosing FHL3 by Western blotting using platelet protein. The amount of Munc13-4 protein expression was compared between platelets and PBMCs (A) and among platelets, $CD8^+$, $CD4^+$, $CD19^+$, and $CD14^+$ cells (B) by Western blotting. A representative result of 5 independent experiments is shown. (C) Six FHL3 patients were diagnosed by Western blotting for Munc13-4 protein using platelets.

obtained by standard density gradient centrifugation was actually derived from the contaminating platelets (Figure 2B).

We performed a NK-cell degranulation assay for every referred sample and found the assay to be defective for every FHL3 patient identified (data not shown). All of the other patients showed a normal release of lysosomal granules by NK cells; however, the analysis could not be performed in some patients because of the extremely low NK-cell number during the acute phase of the disease (data not shown).

We also examined the lysosomal granule release of platelets in 31 patients to determine whether this assay could be used as a screening method for FHL3. Lysosomal exocytosis of FHL3 platelets was partially impaired at steady state, but profound impairment was observed during the acute phase of the disease (Figure 3A-C). This profound impairment was also observed in platelets obtained from some secondary HLH patients during the acute phase (Figure 3B-C). These results indicate that it is difficult to diagnose FHL3 during the acute phase of HLH either by Western blot or by lysosomal degranulation assay.

Table 1. UNC13D gene mutations of FHL3 patients

Patient	Age at onset	Gender	Mutation	Genotype	Predicted effect
P1	14 days	Female	c.1596 + 1G → C	Homo	Splice error
P2	2 months	Male	c.322–1G → A	Hetero	Splice error
			c.990G → C	Hetero	p.Q330H
			c.3193C → T	Hetero	p.R1065X
P3	12 months	Female	c.754–1G → C	Hetero	Splice error
			c.2485delC	Hetero	p.L829fs
P4	4 months	Female	c.754–1G → C	Hetero	Splice error
			c.1799C → T	Hetero	p.T600M
			c.1803C → A	Hetero	p.Y601X
P5	2 months	Female	c.754–1G → C	Hetero	Splice error
			c.1596 + 1G → C	Hetero	Splice error
P6	5 months	Male	ND	ND	ND

Mutations were checked for single nucleotide polymorphisms using the dbSNP Build 132 database from the National Center for Biotechnology Information.

X indicates stop; fs, frame shift; and ND, not determined.

Rapid diagnosis of FHL3 by flow cytometric detection of intraplatelet Munc13-4

To overcome the difficulty in diagnosing FHL3 during the acute phase of HLH, antibodies were raised against the full-length human Munc13-4 protein (supplemental Figure 1) and a new method was developed to detect Munc13-4 protein in platelets by flow cytometry. A total of 35 patients, including 4 with FHL3 (P3-P6), were

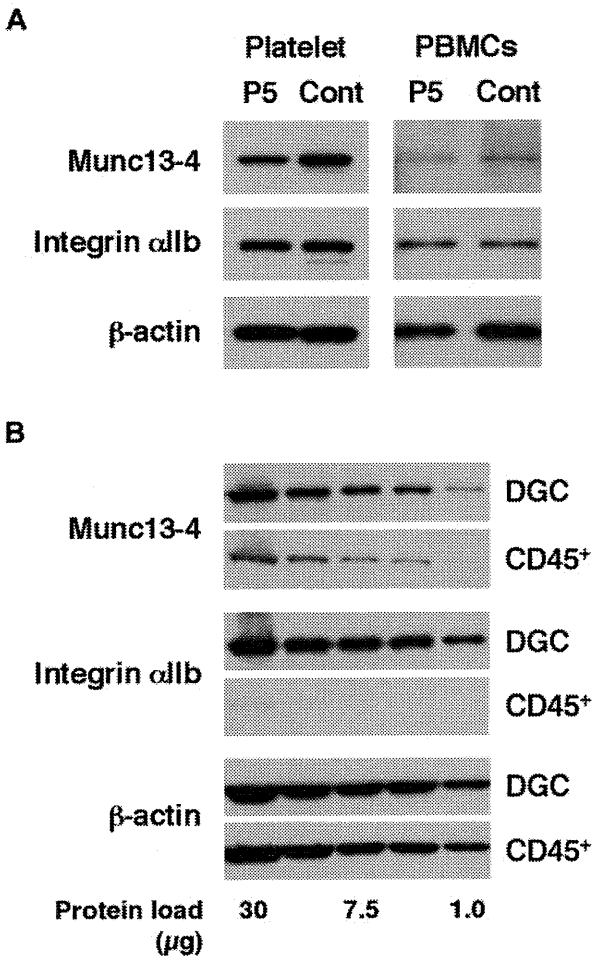

Figure 2. Effect of platelet transfusion on Western blot analysis. (A) Western blotting analysis for Munc13-4 expression using platelets and PBMCs from an FHL3 patient (P5) receiving platelet transfusions during the acute phase of the disease. (B) The expression of Munc13-4 was compared between PBMCs obtained by density gradient centrifugation (DGC) and $CD45^+$ cells obtained by magnetic sorting from healthy controls. A representative result of 3 independent experiments is shown.

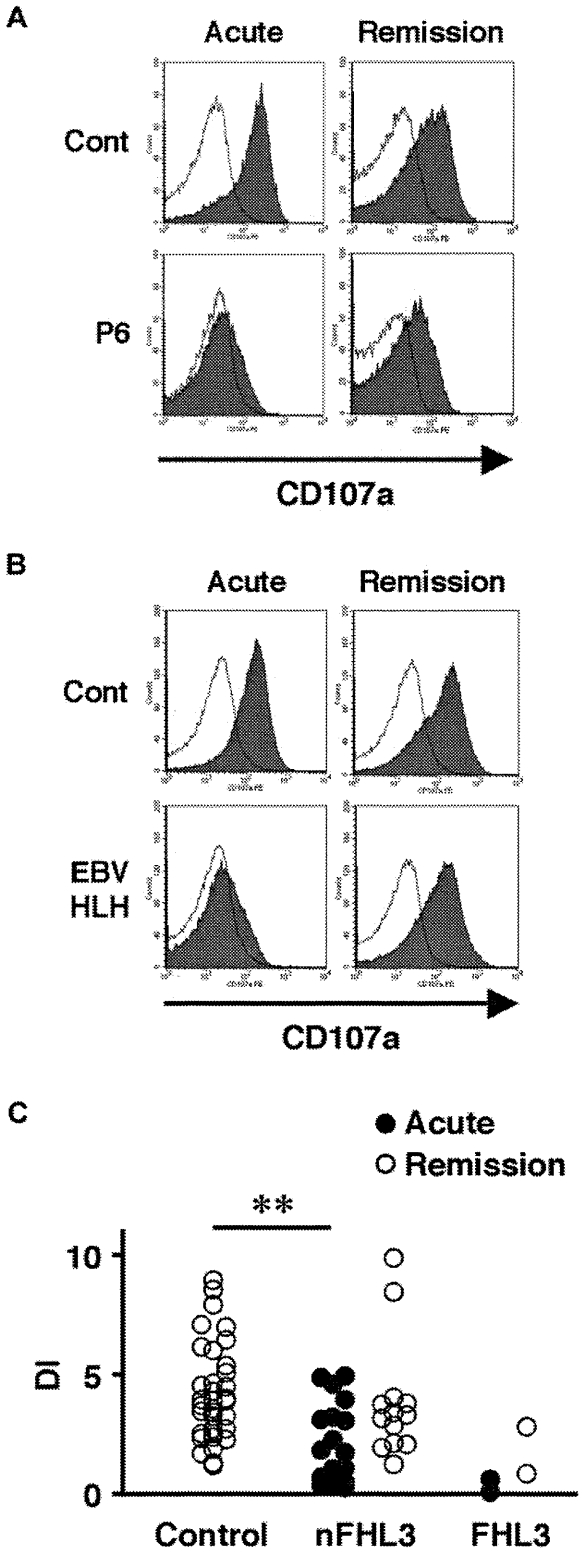

Figure 3. Analysis of lysosomal exocytosis using platelets from HLH patients. Platelets from an FHL3 patient (P6; A) and from a secondary (EBV-associated) HLH patient (B) along with healthy controls were left untreated (open histogram) or were stimulated with thrombin (closed histograms), and the surface expression of CD107a was analyzed by flow cytometry. Analysis was performed during the acute phase of the disease (left column) and after clinical remission (right column). (C) Degranulation index (DI) of platelets from HLH patients during the acute phase (●) and after clinical remission (○). HLH patients with normal NK-cell degranulation and Munc13-4 protein expression by Western blot analysis were defined as non-FHL3 (nFHL3). $^{**}P < .01$ by the Tukey post hoc test.

analyzed using this method. Munc13-4 deficiency was readily detected in all of the FHL3 patients, with a sample volume of < 100 μL of whole blood (Figure 4A-C). Munc13-4 protein was expressed at normal level in the platelets of parents and siblings of FHL3 patients carrying heterozygous *UNC13D* mutations (data not shown). In the FHL3 patient receiving platelet transfusions, flow cytometric analysis revealed bimodal populations of normal and Munc13-4–deficient platelets (P5 in Figure 4A). As shown in Figure 4B, the method was able to clearly identify Munc13-4–deficient platelets in whole blood samples stored at room temperature for 1 week.

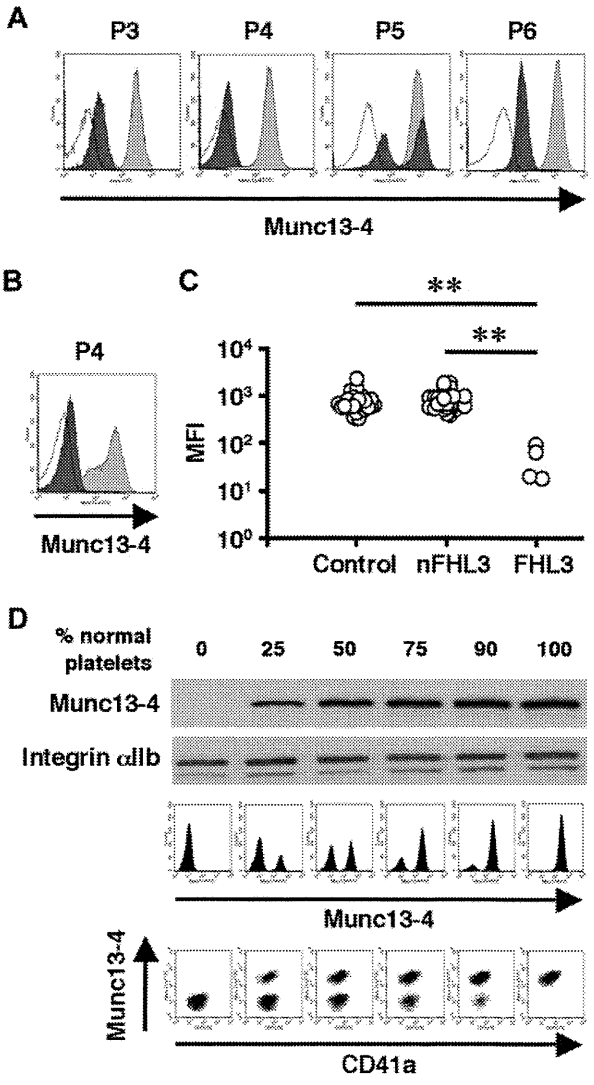

Figure 4. Flow cytometric detection of intraplatelet Munc13-4 protein. Flow cytometric analysis of intraplatelet Munc13-4 expression in 4 FHL3 patients and healthy controls using whole blood samples shipped overnight (A) and in an FHL3 patient (P4) and a healthy control using samples stored at room temperature for a week (B). Dark closed histograms represent platelets from FHL3 patients, whereas light closed histograms represent platelets from healthy controls. Open histograms represent staining with isotype controls. (C) Mean fluorescence intensity (MFI) of intraplatelet Munc13-4 staining for HLH patients and healthy controls. All of the healthy controls (n = 35) were adults. Non-FHL3 (nFHL3) patients (n = 31), as defined in Figure 3, varied in age (2 days-39 years) and included 2 patients with FHL2. Age-related variations in the MFI of Munc13-4 staining were not observed. $^{**}P < .01$ by the Tukey post hoc test. (D) The sensitivities of Western blot and flow cytometric analyses for detecting Munc13-4–deficient platelets were compared.

To determine the sensitivity of the new method, Munc13-4–deficient platelets were mixed with normal platelets at varying ratios. Western blot analysis could not detect Munc13-4–deficient platelets easily, even when the proportion of normal platelets was as low as 25% (Figure 4D). In contrast, flow cytometric analysis easily identified 10% Munc13-4–deficient platelets among 90% normal platelets (Figure 4D), which proved the high sensitivity of the method in diagnosing FHL3.

Discussion

FHL is a rare but life-threatening inherited immune disorder for which mutations in 4 genes have been identified as causative factors. *PRF1* encodes the cytolytic effector protein perforin that forms a pore-like structure in the target cell membrane.[1,12] A mutation in *PRF1* results in FHL2,[7] which accounts for 20%-50% of FHL cases.[4,5] *UNC13D* encodes the protein Munc13-4, which is crucial for the fusion of cytolytic granules to the plasma membrane and the subsequent release of perforin and granzymes.[1,12] Mutations in *UNC13D* result in FHL3,[8] which accounts for 20%-30% of FHL cases.[4,12] FHL4 is caused by mutations in *STX11*, which encodes syntaxin-11.[9] Mutations in *STXBP2*, which encodes Munc18-2, were recently reported to cause FHL5.[10,11] Syntaxin-11 and Munc18-2 also mediate the fusion of cytolytic granules to the plasma membrane.[1,5,12] The ability to screen for FHL2-5 rapidly would facilitate the initiation of life-saving immunosuppressive therapy and the preparation of FHL patients for hematopoietic stem cell transplantation.

In the present study, we found that the Munc13-4 protein is expressed abundantly in platelets (Figure 1A-B). The detection of Munc13-4 protein in platelets by Western blotting (Figure 1C) or flow cytometry (Figure 4A-B) was a reliable screening method to identify FHL3 patients. Munc13-4–deficient platelets were identified easily among normal transfused platelets by flow cytometry, which indicated that this method could be applied to patients who are receiving platelet transfusions during the acute phase of the disease (P5 in Figure 4A). Detection of intraplatelet Munc13-4 was enabled by the use of highly specific antibodies against the full-length human Munc13-4 (supplemental Figure 1).

There is a possibility that FHL3 patients with residual Munc13-4 protein expression could be overlooked by the screening methods described in this study. Most FHL3 patients have mutations that result in the absence or significant reduction of Munc13-4 protein expression,[16,23] as was the case with the patients screened in this study (Figure 1C), which suggests that the mutated Munc13-4 protein is unstable. The NK-cell degranulation assay, which was performed for every referred sample with a sufficient number of NK cells, revealed defective degranulation only in the identified FHL3 patients (date not shown). These results indicate that the majority of mutations in *UNC13D* are likely amenable to rapid detection by the new methods described in this study. Comparative studies on the *UNC13D* genotype, Munc13-4 protein expression, and the lysosomal exocytosis assay must be performed to confirm the reliability of these methods.

It was also investigated whether the analysis of lysosomal release by platelets could be used as an alternative method to screen for FHL3. Profound impairment of lysosomal exocytosis by platelets during the acute phase of the disease and restoration of this impairment after clinical remission was observed in FHL3 and in some secondary HLH patients (Figure 3). It is not clear whether this transient impairment of platelet degranulation is involved in HLH pathogenesis or if it merely reflects in vivo platelet activation by diffuse endothelial damage during the acute phase of the disease that renders them unresponsive to ex vivo stimulation. The release of lysosomal granules by Munc13-4–deficient platelets was impaired only minimally at steady state (Figure 3A and 3C), which is in contrast to a recent study showing the involvement of the Munc13-4 protein in the release of lysosomal granules in mouse platelets.[27] Although the precise reason for this discrepancy is unclear, platelet degranulation is likely to be regulated differentially between species; for example, Munc13-4–deficient mice have bruising and bleeding tendencies[27] that are not commonly associated with human FHL3. Further studies are warranted to elucidate the exocytosis pathways of platelets and their role in the pathophysiology of HLH.

With the development of tools for rapid screening, the diagnostic approach for FHL has changed over the years. Impaired NK cytotoxicity was the first reported signature clinical finding of FHL patients.[13,14] Defective CTL activity was subsequently reported as another hallmark of FHL.[7,8,16,28] However, NK-cell activity is also decreased in some cases of secondary HLH,[15,17-20] and the CTL cytotoxicity assay is not readily accessible to most clinicians. The NK-cell lysosomal exocytosis assay is a comprehensive method to identify patients with a degranulation defect.[10,11,22-24] However, this analysis is not available in some patients with extremely reduced NK-cell numbers, which are often observed during the acute phase of HLH.[19] Although CTLs can be an alternative tool to perform the lysosomal exocytosis assay,[24,28,29] it remains impossible to differentiate FHL3-FHL5.[10,11,23,24] Impairment in these assays warrants the genetic confirmation of FHL, but sequencing all of the candidate genes is not a suitable approach for rapid diagnosis. Flow cytometric detection of perforin expression in NK cells is a reliable and rapid way of identifying patients with FHL2,[21] and the new method described in this study for the detection of Munc13-4 expression in platelets would add to the rapid diagnosis of FHL3.

Platelets could also be used for the screening of FHL4 and FHL5 because they share some granule-transport mechanisms with other types of hematopoietic cells, including CTLs and NK cells.[2,30,31] Indeed, in the present study, both syntaxin-11 and Munc18-2 were expressed abundantly in platelets (data not shown). We are currently using platelet proteins to screen for FHL4-FHL5 by Western blot analysis, although no cases have been found so far because of the extreme rarity of these disorders.

In summary, platelets abundantly express Munc13-4 protein and are a useful tool to screen for FHL3. By detecting intraplatelet Munc13-4 expression by flow cytometry, it is now possible to rapidly screen for FHL3 with a very small sample of whole blood, even in the acute disease phase requiring platelet transfusion. Because platelets share some of their granule transport systems with other types of hematopoietic cells, they could also be used to screen for other types of immune disorders, including FHL4 and FHL5.

Acknowledgments

The authors are grateful to all of the participating patients, their families, and the referring physicians for their generous cooperation in this study.

This study was supported by grants from The Morinaga Foundation for Health and Nutrition; from the Japanese Ministry of

Education, Culture, Sports, Science, and Technology; and from the Japanese Ministry of Health, Labor, and Welfare.

Authorship

Contribution: T.Y., R.N., T.N., H.H., and H.T. designed the research; Y.M., K.I., and M.S. performed the Western blot and flow cytometric analyses; K.O. and O.O. performed the genetic analyses; R.S. and H.H. prepared the anti–Munc13-4 antibodies and started the FHL3 screening; Y.M., T.Y., R.S., K.I., H.S., J.A., N.T., T.K., R.N., E.I., T.N., H.H., and T.H. analyzed and discussed the results; and Y.M., T.Y., and T.H. wrote the manuscript.

Conflict-of-interest disclosure: The authors declare no competing financial interests.

Correspondence: Takahiro Yasumi, Department of Pediatrics, Kyoto University Graduate School of Medicine, 54 Kawahara-cho, Shogoin, Sakyo-ku, Kyoto, 606-8507 Japan; e-mail: yasumi@kuhp.kyoto-u.ac.jp or Hisanori Horiuchi, Department of Molecular and Cellular Biology, Institute of Development, Aging and Cancer, Tohoku University, 4-1 Seiryo-machi, Aoba-ku, Sendai 980-8575 Japan; e-mail: horiuchi@idac.tohoku.ac.jp.

References

1. Fischer A, Latour S, de Saint Basile G. Genetic defects affecting lymphocyte cytotoxicity. *Curr Opin Immunol.* 2007;19(3):348-353.
2. Hong W. Cytotoxic T lymphocyte exocytosis: bring on the SNAREs! *Trends Cell Biol.* 2005; 15(12):644-650.
3. Ménasché G, Feldmann J, Fischer A, de Saint Basile G. Primary hemophagocytic syndromes point to a direct link between lymphocyte cytotoxicity and homeostasis. *Immunol Rev.* 2005;203: 165-179.
4. Janka GE. Familial and acquired hemophagocytic lymphohistiocytosis. *Eur J Pediatr.* 2007; 166(2):95-109.
5. Gupta S, Weitzman S. Primary and secondary hemophagocytic lymphohistiocytosis: clinical features, pathogenesis and therapy. *Expert Rev Clin Immunol.* 2010;6(1):137-154.
6. Créput C, Galicier L, Buyse S, Azoulay E. Understanding organ dysfunction in hemophagocytic lymphohistiocytosis. *Intensive Care Med.* 2008; 34(7):1177-1187.
7. Stepp S, Dufourcq-Lagelouse R, Le Deist F, et al. Perforin gene defects in familial hemophagocytic lymphohistiocytosis. *Science.* 1999;286(5446): 1957-1959.
8. Feldmann J, Callebaut I, Raposo G, et al. Munc13-4 is essential for cytolytic granules fusion and is mutated in a form of familial hemophagocytic lymphohistiocytosis (FHL3). *Cell.* 2003; 115(4):461-473.
9. zur Stadt U, Schmidt S, Kasper B, et al. Linkage of familial hemophagocytic lymphohistiocytosis (FHL) type-4 to chromosome 6q24 and identification of mutations in syntaxin 11. *Hum Mol Genet.* 2005;14(6):827-834.
10. zur Stadt U, Rohr J, Seifert W, et al. Familial hemophagocytic lymphohistiocytosis type 5 (FHL-5) is caused by mutations in Munc18-2 and impaired binding to syntaxin 11. *Am J Hum Genet.* 2009; 85(4):482-492.
11. Côte M, Ménager M, Burgess A, et al. Munc18-2 deficiency causes familial hemophagocytic lymphohistiocytosis type 5 and impairs cytotoxic granule exocytosis in patient NK cells. *J Clin Invest.* 2009;119(12):3765-3773.
12. Cetica V, Pende D, Griffiths GM, Aricò M. Molecular basis of familial hemophagocytic lymphohistiocytosis. *Haematologica.* 2010;95(4):538-541.
13. Perez N, Virelizier JL, Arenzana-Seisdedos F, Fischer A, Griscelli C. Impaired natural killer activity in lymphohistiocytosis syndrome. *J Pediatr.* 1984;104(4):569-573.
14. Aricò M, Nespoli L, Maccario R, et al. Natural cytotoxicity impairment in familial haemophagocytic lymphohistiocytosis. *Arch Dis Child.* 1988;63(3): 292-296.
15. Schneider EM, Lorenz I, Müller-Rosenberger M, Steinbach G, Kron M, Janka-Schaub GE. Hemophagocytic lymphohistiocytosis is associated with deficiencies of cellular cytolysis but normal expression of transcripts relevant to killer-cell-induced apoptosis. *Blood.* 2002;100(8): 2891-2898.
16. Ishii E, Ueda I, Shirakawa R, et al. Genetic subtypes of familial hemophagocytic lymphohistiocytosis: correlations with clinical features and cytotoxic T lymphocyte/natural killer cell functions. *Blood.* 2005;105(9):3442-3448.
17. Schneider EM, Lorenz I, Walther P, Janka-Schaub GE. Natural killer deficiency: a minor or major factor in the manifestation of hemophagocytic lymphohistiocytosis? *J Pediatr Hematol Oncol.* 2003;25(9):680-683.
18. Grom AA, Villanueva J, Lee S, Goldmuntz EA, Passo MH, Filipovich A. Natural killer cell dysfunction in patients with systemic-onset juvenile rheumatoid arthritis and macrophage activation syndrome. *J Pediatr.* 2003;142(3):292-296.
19. Grom AA. Natural killer cell dysfunction: A common pathway in systemic-onset juvenile rheumatoid arthritis, macrophage activation syndrome, and hemophagocytic lymphohistiocytosis? *Arthritis Rheum.* 2004;50(3):689-698.
20. Horne A, Zheng C, Lorenz I, et al. Subtyping of natural killer cell cytotoxicity deficiencies in haemophagocytic lymphohistiocytosis provides therapeutic guidance. *Br J Haematol.* 2005;129(5): 658-666.
21. Kogawa K, Lee SM, Villanueva J, Marmer D, Sumegi J, Filipovich AH. Perforin expression in cytotoxic lymphocytes from patients with hemophagocytic lymphohistiocytosis and their family members. *Blood.* 2002;99(1):61-66.
22. Alter G, Malenfant JM, Altfeld M. CD107a as a functional marker for the identification of natural killer cell activity. *J Immunol Methods.* 2004; 294(1-2):15-22.
23. Marcenaro S, Gallo F, Martini S, et al. Analysis of natural killer-cell function in familial hemophagocytic lymphohistiocytosis (FHL): defective CD107a surface expression heralds Munc13-4 defect and discriminates between genetic subtypes of the disease. *Blood.* 2006;108(7): 2316-2323.
24. Bryceson YT, Rudd E, Zheng C, et al. Defective cytotoxic lymphocyte degranulation in syntaxin-11 deficient familial hemophagocytic lymphohistiocytosis 4 (FHL4) patients. *Blood.* 2007;110(6): 1906-1915.
25. Shirakawa R, Higashi T, Tabuchi A, et al. Munc13-4 is a GTP-Rab27-binding protein regulating dense core granule secretion in platelets. *J Biol Chem.* 2004;279(11):10730-10737.
26. Febbraio M, Silverstein RL. Identification and characterization of LAMP-1 as an activation-dependent platelet surface glycoprotein. *J Biol Chem.* 1990;265(30):18531-18537.
27. Ren Q, Wimmer C, Chicka MC, et al. Munc13-4 is a limiting factor in the pathway required for platelet granule release and hemostasis. *Blood.* 2010; 116(6):869-877.
28. Nagai K, Yamamoto K, Fujiwara H, et al. Subtypes of familial hemophagocytic lymphohistiocytosis in Japan based on genetic and functional analyses of cytotoxic T lymphocytes. *PLoS ONE.* 2010;5(11):e14173.
29. Rohr J, Beutel K, Maul-Pavicic A, et al. Atypical familial hemophagocytic lymphohistiocytosis due to mutations in UNC13D and STXBP2 overlaps with primary immunodeficiency diseases. *Haematologica.* 2010;95(12):2080-2087.
30. Stinchcombe J, Bossi G, Griffiths G. Linking albinism and immunity: the secrets of secretory lysosomes. *Science.* 2004;305(5680):55-59.
31. Ren Q, Ye S, Whiteheart SW. The platelet release reaction: just when you thought platelet secretion was simple. *Curr Opin Hematol.* 2008;15(5): 537-541.